The version of record:

Vannozzi, A. et al *Combinatorial regulation of stilbene synthase genes by WRKY and MYB transcription factors in grapevine (Vitis vinífera L.)* in Plant & cell physiology, vol. 59, issue 5 (May 2018), p. 1043-1059

Is available online at: DOI 10.1093/pcp/pcy045

Title: Combinatorial Regulation of Stilbene Synthase Genes by WRKY and MYB Transcription Factors in Grapevine (*Vitis vinifera* L.)

Running head: WRKYs and MYBs control stilbene synthesis in grape

Corresponding author: Alessandro Vannozzi; Department of Agronomy, Food, Natural resources, Animals, and Environment (DAFNAE), University of Padova, 35020 Legnaro, Italy; Tel: +393920094888; Email address: alessandro.vannozzi@unipd.it

Subject areas: Regulation of gene expression; Genomics, system biology and evolution

Number of colour figures: 7

Number of tables: 1

Number of Supplementary material: 7

Title: Combinatorial Regulation of Stilbene Synthase Genes by WRKY and MYB Transcription Factors in Grapevine (*Vitis vinifera* L.)

Running head: WRKYs and MYBs control stilbene synthesis in grape

AlessandroVannozzi[1*+]; Darren Chern Jan Wong[2+]; Janine Höll[3]; Ibrahim Hmmam[1#]; José Tomás Matus[4]; Jochen Bogs[3]; Tobias Ziegler[3]; Ian Dry[5]; Gianni Barcaccia[1]; Margherita Lucchin[1]

[1]Department of Agronomy, Food, Natural resources, Animals, and Environment (DAFNAE), University of Padova, 35020 Legnaro, Italy.

[2]Ecology and Evolution, Research School of Biology, Australian National University Acton, ACT 2601, Australia.

[3]Centre for Organismal Studies Heidelberg, University of Heidelberg, 69120 Heidelberg, Germany.

[4]Centre for Research in Agricultural Genomics (CRAG) CSIC-IRTA-UAB-UB, Barcelona 08034, Spain.

[5]CSIRO Agriculture & Food, Urrbrae, SA 5064, Australia.

*: Corresponding Author; Email: alessandro.vannozzi@unipd.it

+: Equal contribution

#: current address: Department of Pomology, Faculty of Agriculture, Cairo University, 12613 Giza, Egypt

Abbreviations: AI, aliphatic index; bHLH, basic helix-loop-helix; CHS, chalcone synthase; CRE, *cis*-regulatory element; EF1, elongation factor 1; ERF, ethylene responsive factor; FC, fold change; FDR, false discovery rate; GCN, gene coexpression network; GRAVY, grand average of hydropathicity; GRsPaV, grapevine rupestris stem pitting-associated virus; GUS, β-glucuronidase; HsF, heat shock transcription factor; II, protein instability index; JA, jasmonic acid; LSD, least significant difference; LUC, luciferase; MR, mutual ranking; MUSCLE, multiple sequence comparison by log-expectation; MW, molecular weight; NGS, next generation sequencing; PCC, Pearson correlation coefficient; pI, isoelectric point; PKS, polyketide synthase; qPCR, quantitative PCR; RNA-seq, RNA sequencing; SA, salicylic acid; SE, standard error; SRA, sequence read archive; STS, stilbene synthase; TF, transcription factor; TFBS, transcription factor binding site; TFDB, transcription factor database; TPS, terpene synthase; TSS, transcription starting site; UV-C, ultraviolet C; UTR, untranslated region.

Abstract

Stilbene synthase (STS) is the key enzyme leading to the biosynthesis of resveratrol. Recently we reported two R2R3-MYB transcription factors (TFs) that regulate the stilbene biosynthetic pathway in grapevine: *VviMYB14* and *VviMYB15*. These genes strongly co-express with *STS*s under a range of stress and developmental conditions, in agreement with the specific activation of *STS* promoters by these TFs. Genome-wide gene co-expression analysis using two separate transcriptome compendia based on microarray and RNA-Seq data revealed that WRKY TFs were the top TF family correlated with STS genes. On the basis of correlation frequency, four WRKY genes, namely *VviWRKY03*, VviWRKY24, *VviWRKY43* and *VviWRKY53*, were further shortlisted and functionally validated. Expression analyses under both unstressed and stressed conditions, together with promoter-luciferase reporter assays, suggested different hierarchies for these TFs in the regulation of the stilbene biosynthetic pathway. In particular, VviWRKY24 seems to act as a singular effector in the activation of the *VviSTS29* promoter, while VviWRKY03 acts through a combinatorial effect with VviMYB14, suggesting these two regulators may interact at the protein level as previously reported in other species.

Keywords: Gene co-expression, Network, Resveratrol, *Vitis vinifera*

Introduction

In the last decade, the availability of an accurate grapevine (*Vitis vinifera* L.) genome assembly (Jaillon et al. 2007), together with the release of a detailed annotation, namely 12X.v2 (Vitulo et al. 2014) (recently updated with the release of VCost.v3; Canaguier et al. 2017) has been accompanied with a remarkable rise in genomic and transcriptomic data available for this species. As a matter of fact, grapevine represents one of the most representative examples of how next generation sequencing technology (NGS) massively impacts plant genomics and plant molecular biology (Fabres et al. 2017). Recently, network analyses have contributed to an increased understanding of the regulatory mechanisms that control grape berry development and composition (Ali et al 2010). In this sense, and based on the notion that genes involved in similar or related processes may exhibit similar expression patterns over a range of experimental conditions, an increasing number of studies have used gene co-expression networks to find common pathways and putative targets for transcription factors related to berry development and secondary metabolism (reviewed by Wong and Matus 2017).

The value of exploiting omics data in *Vitis* species relies on the fact that, wild and cultivate grapevines produce a vast array of chemical compounds many of which are related to wine quality and have been implicated in promoting human health (Wong and Matus 2017). Among these, stilbenes, a class of phenolic secondary metabolites characterized by the presence of a 1,2-diphenylethylene backbone, have been increasingly studied over the last decade because of their nutraceutical properties, with considerable potential in drug research (e.g. anticancerinogenesis; Ali et al. 2010, Pangeni et al. 2014, Weiskirchen and Weiskirchen 2016) and also with important roles in the protection of plants against pests, pathogens and abiotic stresses (Chong et al. 2009, Jeandet et al. 2010).

Together with flavonoids, stilbenes belong to the plant polyketide class representing a major group of phenylpropanoids derived from the extension of the activated form of coumaric acid with three acetyl moieties. Apart from the *Vitaceae*, current literature indicates that stilbenes are produced by a polyphyletic group of species limited to approximately 50 plant families including dicotyledons, monocotyledons, conifers, liverworts, and ferns (Pangeni et al. 2014, Weiskirchen and Weiskirchen 2016). Despite the multiplicity of stilbene units found in different plant species (Shen et al. 2009, Rivière et al. 2012), most of them (including those in grapevine), are derivatives of the basic unit trans-resveratrol (3,5,4'-trihydroxy-*trans*-stilbene). Resveratrol has been the subject of numerous research studies since it was postulated to have a role in the so-called 'French paradox', which refers to the observation that French people have a relatively low incidence of coronary heart disease, despite having a diet rich in saturated fats. In fact, hundreds of subsequent studies have reported that this compound can prevent or slow down a variety of diseases, including cancer, diabetes, as well as extend the

lifespan of various organisms (Pengeni et al. 2014, Weiskirchen and Weiskirchen 2016, Tzai et al. 2017). The biosynthesis of resveratrol is achieved through a small branch of the general phenylpropanoid pathway and can be considered as a competitive extension of the flavonoid branch (Vannozzi et al. 2012). Stilbene synthase (STS) is the key enzyme leading to the production of resveratrol and belongs to the chalcone synthase (CHS) superfamily of type III polyketide synthases (PKSs; Chong et al. 2009). In grapevine, an analysis of the *STS* multigenic family based on both the PN40024 and PN ENTAV 115 genomes (Jaillon et al. 2007, Velasco et al. 2007) led to the identification of 48 putative *STS* gene sequences, with at least 33 encoding full length STS proteins (Vannozzi et al. 2012).

Two R2R3-type V-myb myeloblastosis viral oncogene homolog (MYB) transcription factors (TFs) have been shown to regulate stilbene biosynthesis in the grapevine (Höll et al. 2013). These R2R3-MYB-type TFs, designated as *MYB14* and *MYB15*, are found to be strongly co-expressed with certain *STS* genes in different grapevine organs in response to biotic and abiotic stress including downy mildew (*Plasmopara viticola*) infection, mechanical wounding and exposure to UV-C irradiation (Höll et al. 2013). The expression of *MYB14* and *MYB15,* is also correlated with the accumulation of *trans*-piceid in developing grape berries (Höll et al. 2013). Furthermore, grapevine cell cultures transiently expressing *STS promoter::luciferase* reporter constructs showed considerable induction of the activities of the promoters of *STS29* and *STS41*, whenever co-transfected with *MYB14* and *MYB15*. The involvement of these TFs in the regulation of stilbene biosynthesis *in planta* was demonstrated using transgenic grapevine hairy roots overexpressing *MYB15*, which showed an increased accumulation of *trans*-piceid, associated with an up-regulation of *STS29* and *STS41* transcription levels. Furthermore, Fang et al. (2014) demonstrated that the variation in expression of *MYB14* correlated with the variation in resveratrol content in two grapevine cultivars (*Vitis monticola* x *Vitis riparia* - high resveratrol producer and *V. vinifera* - low resveratrol producer) and, using a one-hybrid yeast assay, showed that MYB14 directly interacts with the *STS* promoter *in vitro*. This study also demonstrated that a transient overexpression of *MYB14* could activate *STS* expression in grapevine leaves and that its overexpression in transgenic *Arabidopsis* could activate GUS expression driven by a *STS* promoter. Wong et al. (2016) showed that these two TF genes shared close similarity (in sequence and expression) with *MYB13*, suggesting that, in addition to MYB14 and MYB15, MYB13 may be also involved in the transcriptional regulation of at least some *STS* genes in grapevine.

Recently, a composite network for STS regulation was constructed with the aim of illustrating different approaches of data integration for network analysis in grapevine (Wong and Matus. 2017). Using publicly available berry-specific RNA-Seq data, the authors overlapped gene co-expression networks with the presence of promoter *cis*-binding elements (CRE), microRNAs and long non-coding RNAs. As a result, a systems-level STS

regulatory network was inferred from the context of berry development and ripening. However, this network still needs to be demonstrated to operate *in planta.*

The present study was aimed at extending the current knowledge pertaining to the regulation of stilbene biosynthesis in grapevine, by identifying and characterizing TFs, other than R2R3-MYBs, that are potentially involved in the regulation of the stilbene biosynthesis. To do this we performed a large-scale co-expression analysis identifying novel candidate TFs belonging to different gene families. Amongst these was the WRKY TF family, which represented one of the most enriched families in terms of correlation frequencies with *STS* genes. Based on network connectivity properties, we selected *WRKY03*, *WRKY24*, *WRKY43* and *WRKY53* for further examination. Expression analyses of grapevine tissues under different stress and unstressed conditions, together with functional reporter gene assays suggest different roles for these TFs in the regulation of the *STS* pathway.

Results and Discussion

An integrated co-expression network confirms and identifies potential regulators of *STS* expression

The flavonoid biosynthetic pathway is considered one of the best systems available for studying the regulation of gene expression in plants (Davies and Schwinn 2003) and also in grapevine (*V. vinifera* L.), where it represents one of the most studied crops in this regard. Although many TFs involved in the regulation of specific flavonoid structural genes in grapes have been identified, there is evidence to suggest that novel regulators remain to be characterized (Wong and Matus 2017). To investigate this, we first constructed two independent global gene co-expression networks (GCNs) based on mutual ranking (MR) using datasets produced with Next Generation Sequencing (NGS) (21 experiments, 235 conditions averaged from 654 RNA-Seq assays; Supplementary Table S1) and microarrays (23 experiments, 359 conditions averaged from 914 arrays; Supplementary Table S1). The choice of the MR index over Pearson correlation coefficient (PCC) as the preferred co-expression measure in this study is supported by previous studies showing that the latter is more robust to outliers and has higher predictive power in gene function inference compared to correlation-based metrics (Obayashi et al. 2009).

For the construction of a robust *STS* GCN, we first determined the optimal threshold of neighborhood size, *k* aimed at maximizing the number of genes included while keeping potential false-positives inclusions to a minimum. We began by investigating the relationship of different *k* thresholds (e.g. *k* of 100 to 1000) on the distribution of PCC values for each member of the grapevine *STS* family described in Vannozzi et al. (2012) in the microarray and NGS *STS* GCNs separately (See materials and methods). At a *k* of 300, a widely-adopted limit for establishing a practical size of co-expressed genes lists for functional validation (Obayashi and Kinoshita, 2010, Aoki et al. 2016), the median PCC value in the observed microarray *STS* and random

microarray GCN was 0.57 and 0.29, respectively (Supplementary Figure 1A). The same *k* in the observed *STS* and random NGS GCN showed a median PCC of 0.67 and 0.01, respectively (Supplementary Figure 1B). In the microarray GCN, overlaps in PCC distribution between the observed *STS* and random GCN was minimal when $k \leq 300$. However, establishment of an appropriate *k* is not as straightforward for the *STS* NGS GCN. The observed PCC distribution in the latter was generally high (PCC between 0.64 and 0.66) even at high *k* ranges (e.g. $k > 500$) while the PCC distribution in random GCNs were often close to 0 across all *k* ranges, complicating the selection of an appropriate *k* with this approach. Several studies have shown that RNA-seq derived PCC GCN can have skewed PCC density distributions (in both negative and/or positive directions) and that the PCC measure is often sensitive to differences in sample sizes (Giorgi et al. 2013, Huang et al. 2017, Wisecaver et al. 2017). For these reasons, the rank of correlations (e.g. MR) are often preferred in recent co-expression studies.

As an additional measure to guide the choice of choosing the appropriate *k* threshold, we established the statistical significance of MR values in the global microarray and NGS GCN, by analyzing the distribution of MR values over 1,000 permutations of the respective dataset. The analysis revealed that MR ≤ 383 and ≤ 417 are significant at $P < 0.01$, for the global microarray and NGS GCN, respectively (Supplementary Figure 1C-D). These results are comparable with earlier studies across a wide range of plant GCNs constructed with correlation-ranked metrics at stringent thresholds (e.g. $P < 0.01$) (Wong et al. 2014, Wong et al. 2013, Mutwil et al. 2011). Nonetheless, weaker MR (e.g. MR < 1000) observed at *P* between 0.01 and 0.05 in both GCNs (Supplementary Figure 1C-D) may still be statistically reliable and biologically meaningful (Obayashi and Kinoshita, 2010, Aoki et al. 2016). By combining clues garnered from both statistical approaches, we determined that a top *k* threshold of 200 would be suited for the construction of a robust *STS* GCN from both platforms. This is supported by the fact that nearly all observed MR values are significant at $P < 0.01$ (with the exception of 123 of 9000 co-expression gene pairs in the NGS *STS* GCN; Supplementary Table S2) and a minimal overlap of PCC distribution (across quartiles) between the observed and permuted GCN (Supplementary Figure 1C-D), in both platforms. Furthermore, a *k* of 200 is within reasonable limits for designing functional studies (Obayashi and Kinoshita, 2010, Aoki et al. 2016). Similar thresholds have also been used in prioritizing candidate genes in recent grape functional studies (e.g. top100 for microarray co-expressions in Wong et al. 2016, and top300 for RNA-seq co-expressions in Loyola et al. 2016 and Sun et al. 2018).

By merging the two independent STS co-expression modules obtained from both platforms (*k* of 200) into a combined GCN (Supplementary Table S2), we hypothesized that an integrated STS GCN would hold more biologically meaningful co-expression relationships as GCNs constructed from different platforms have the potential to highlight additional functional categories and co-expression relationships (Giorgi et al. 2013). To

assess TF-STS co-expression, we kept only those TF accessions corresponding to predicted grapevine TFs based on the Plant transcription factor database (Plant TFDB; Jin et al. 2017), encompassing 1,256 grapevine TFs distributed among 58 families. In addition, as dense connections between *STS* genes are generally observed in the *STS* GCN (Supplementary Table S2), we hypothesized that *bona fide* regulatory genes involved in *STS* regulation should be frequently co-expressed with multiple *STS* members. As such, we only considered those TFs showing a node degree higher than or equals to 5, i.e. those TFs correlated with at least 5 *STS* genes (10% of total grapevine STS). A list of all top200 STS-related TFs identified independently by the degree is reported in Supplementary table S3. Initial inspection of the exclusive filtered STS-TF CGN showed a strong correlation between 42 *STSs* and 31 TFs, connected by 569 edges (Fig. 1).

Shared edges between RNA-Seq and microarray networks accounted for 75.8% of the total number of edges and 63.8 % and 63.5% of the total microarray and RNA-Seq specific edges, respectively. Within the whole STS-TF GCN, we identified TFs belonging to 8 different families. The most highly represented family comprised the WRKY TFs, with 10 genes (30% of all TFs in the GCN), followed by Ethylene Responsive Factors (7 genes; 23.3%), MYBs (6 genes; 20%), NACs (4 genes; 13.3%), GRASs (2; 6.6%), C2H2, HSF and bHLH (1 gene; 3.3%). Table 1 provides a list of all the TFs co-expressed with *STS* genes and represented in the GCN.

Considering the contribution of edges from both datasets, nodes belonging to the shared-interaction module showed a higher number of interactions with *STSs* (Fig. 1) compared to nodes belonging exclusively to the microarray or RNA-Seq modules. This is the case of *MYB14* (VIT_07s0005g03340), the TF with the highest number of interactions, showing up to 72 edges. *MYB15* is another direct regulator of *STS* transcription (Höll et al. 2013) that appeared within the top200 *STS*-co-expressed genes. Differing from its paralog (both genes belong to R2R3-MYB Subgroup 2), *MYB15* was represented only within the microarray-interaction module, and the number of edges was much lower compared to *MYB14*. This reveals a potential limitation of the GCN approach as the network output can be influenced by the type of experimental conditions used in GCN construction (Usadel et al. 2009) or that the majority of experimental conditions used to generate the RNA-Seq and microarray datasets do not constitute tissues and treatments in which MYB15 has a functional role.

APETALA2/ethylene response factor (*AP2*/*ERF*) transcription factor TFs were also highly represented in the GCN including *VvERF098* (VIT_07s0005g03220), *VvERF112* (VIT_01s0150g00120), *VvERF113* (VIT_07s0031g01980) and *VvERF114* (VIT_18s0072g00260), all belonging to the group X ERF subfamily (Licausi et al. 2010). The members of this ERF subfamily are involved in the plant response to abiotic stresses, including drought and salinity (Fujimoto 2000) and they are expected to be involved in gene regulation under stress conditions involving both ethylene-dependent and -independent pathways (Mizoi et al. 2012). As a matter

of fact, grapevine *STS* genes have been previously demonstrated to be induced in grapevine leaves following treatment with ethepon, an ethylene releasing compound (Belhadj et al. 2008, Becatti et al. 2014), suggesting the signalling pathway related to this hormone could be involved in the activation of the plant stress-response related to stilbene accumulation. This observation, together with the presence of other TFs such as AP2/ERFs within the GCN, leaves open the possibility that the stilbene biosynthetic pathway could be regulated by many different TFs and hormone signalling pathways. Indeed, recent surveys show various AP2/ERF TF binding sites (TFBS) are present within the 1kb promoter region of many grapevine *STS* promoters (Wong and Matus, 2017).

The GCN analysis also identified genes involved in plant stress responses that represent interesting candidates for further analyses. For example, the second largest node in term of degree within the shared-interaction module was VIT_08s0007g08750, a gene that encodes the heat shock transcription factor (HsF), *VviHSFA3a*, one of 19 *HsF* genes predicted within the grapevine genome (Hu et al. 2016). Plant HsF proteins function as TFs regulating the expression of heat shock proteins and other general stress related genes such as the non-chaperone encoding genes *GOLS1* (galactinol synthase 1) or *APX2* (ascorbate peroxidase 2) (Scharf et al. 2012). *VviHSFA3a* belongs to the grapevine *HsF* subgroup A, and was recently demonstrated to be highly responsive to ethylene treatments in *V. pseudoreticulata* (*VpHsf3a*; Hu et al. 2016). This is an interesting observation considering the high number of ethylene responsive factors (ERFs) genes that we identified in the co-expression analysis and the fact that also grape *STSs* are also known to be induced by ethylene (Belhadj et al., 2008). HsFs play pivotal roles in adaptation to heat stress and other stress stimuli including cold, salt, drought, and oxidative stresses (Hu et al., 2016). Many of these abiotic stresses also cause the induction *STS* genes (Vannozzi et al. 2012, Corso et al. 2015).

Another gene of interest identified in the shared-interaction module is VIT_11s0016g02070 which encodes a basic helix-loop-helix (bHLH) protein. The bHLH proteins are a superfamily of TFs that are important regulatory components of many transcriptional complexes, controlling processes such as regulation of flavonoid biosynthesis, floral organogenesis, hormone and light signaling responses and epidermal cell fate determination such as trichome, root hair and stomata formation (Toledo-Ortiz 2003, Sema 2007). It has been demonstrated in various species including maize (*Zea mays*), petunia (*Petunia hybrida*), snapdragon (*Antirrhinum majus*), Arabidopsis (*Arabidopsis thaliana*) and grapevine that MYC-like bHLHs generally interact with R2R3-MYB and WD40 proteins to regulate structural genes involved in flavonoid metabolism (reviewed in Chezem and Clay 2016). In grapevine, VviMYC1, one of the predicted 115 bHLHs based on the Plant TFdb (Jin et al. 2017) has been demonstrated to regulate the anthocyanin and proanthocyanidin pathways by interacting with different flavonoid R2R3-MYB activators (Hichri et al. 2010, Matus et al. 2017) and repressors (Cavallini et al. 2015).

Although our previous research suggested that regulation of stilbene biosynthesis in grapevine by R2R3-MYB TFs was bHLH-independent (Höll et al. 2013), we detected a high level of co-expression between *VIT_11s0016g02070*, *VvSTSs* and *VviMYB14/15* (both in term of PCC and degree). Further work needs to be undertaken to determine the potential role of VIT_11s0016g02070 in the direct or indirect regulation of stilbene biosynthesis.

Potential dual regulation of *STS* by MYB and WRKY transcription factors

The strong co-expression relationships present in the integrated TF-STS GCN is also exemplified by a highly modular GCN between these TFs (Fig. 2). The inferred TF-TF GCN contained 31 genes connected by 191 edges and was organized in three densely connected modules consisting of 13 (module 1), 11 (module 2), and 7 (module 3) genes. The analysis confirmed known and putative *STS* regulators such as *MYB14*, *MYB15*, and *MYB13,* all partitioned to Module 1, with *MYB14* having the highest node degree connecting 9 members module 1, but also to others (i.e. 6 members of module 2, and 3 members of module 3). Meanwhile, three of the four WRKY TFs partitioned to module 2 such as *WRKY02* (15 TFs/genes), *WRKY23* (12 TFs/genes), and *WRKY43* (11 TFs/genes) were also among the top 10 TFs sharing the highest connectivity in the network. The presence of multiple modules with overlapping connectivity also suggests the presence of several regulatory networks that may function in controlling both unique and/or overlapping sets of *STSs*. The high level of connectivity common with *MYB14* and several WRKYs lead us to hypothesize a strong likelihood of combinatorial and synergistic regulation of grapevine *STS* genes by members of these two TF families.

Phylogenetic analysis of WRKY genes highly co-regulated with STS genes

Based on our GCN analysis, genes encoding WRKY (12 genes; 10 with degree > 5) is the top TF family connecting *STS* genes irrespective of the platforms used in the network construction (Fig. 1), suggesting that regulation of *VvSTS* genes could be orchestrated by WRKY TFs. This hypothesis is reinforced by the observation that WRKY cis-regulatory elements (CREs) are found in the promoters of many VvSTS members (Wong and Matus, 2017).

WRKY genes are classified into three main groups (I, II and III) based on the number of WRKY domains and the pattern/position of their zinc finger motifs (Eugelm et al. 2000). Group I WRKYs typically contain two WRKY domains whereas group II and group III members contain a single WRKY domain. Group II WRKYs can be further sub-divided into five subgroups: IIa, IIb, IIc, IId, and IIe (Zhang et al. 2005). Based on phylogenetic analysis of the grapevine WRKY family classification performed by Wang et al. (2014) the WRKY genes found

to be co-expressed with *STS* belong mainly to the WRKY subgroup II (Fig. 3A, Table 1), with four genes belonging to group IIb (*VviWRKY02*, *VviWRKY39*, *VviWRKY29*, and *VviWRKY53*), three genes belonging to group IIc (*VviWRKY03*, *VviWRKY43*, and *VviWRKY11*), and two genes belonging to group IIe (*VviWRKY4* and *VviWRKY30*). Only one co-expressed WRKY TF was found to belong to group I (*VviWRKY24*).

Amongst candidate WRKY TFs, we focused our investigation on four genes, namely *VviWRKY03, VviWRKY24*, *VviWRKY43* and *VviWRKY53. VviWRKY03* and *VviWRKY24* were the top two candidates frequently correlated with *STS* gene expression in the RNA-seq compendia while *VviWRKY43* and *VviWRKY53* were among the top three inferred from the microarray compendia (see Fig. 1). These four candidates are also uniquely positioned across all three modules in the integrated TF-TF GCN (Fig. 2): *VviWRKY03* in module 1 along with the known *STS* regulators (*VviMYB14 and VviMYB5*), *VviWRKY53* in module 2, and *VviWRKY24* and *VviWRKY43* in module 3, the module containing the highest number of WRKY TFs. To provide additional support for this selection, phylogenetic analyses of deduced protein sequences of *VviWRKY43* and VviWRKY03 show them to be most closely related to AtWRKY75, sharing 48% and 53% amino acid identity, respectively. Both genes have similar genomic organizations, containing one single intron (phase 2), and encoding for small proteins (189 aa and 182 aa, respectively). *VviWRKY53*, whose closest homolog in the Arabidopsis genome is *AtWRKY72* (36% amino acid identity), possess five "phase 0" introns and encode for a much larger protein (605 aa) (Fig. 3C). Finally, VviWRKY24 is the orthologue of AtWRKY33, encoding a 552 aa protein. Sequence analysis of these VviWRKYs using PSORT program (Nakai et al. 1999) confirmed the presence of putative nuclear localization signals in all the TFs considered (RKPR for both VviWRKY03 and VviWRKY43 at position 83; PTKKKVE for VvWRKY24 at position 261, PAKRCRV for VviWRKY53 at position 240).

Figure 3B illustrates the results of a phylogenetic analysis based on the predicted translation product of *WRKY* genes identified to be co-expressed with *STS* genes in our GCN, together with WRKY TFs which have already been functionally characterized in grapevine or in other plant species. Interestingly, 27 WRKYs enclosed in the phylogenetic analysis are involved in the regulation of secondary metabolism including many branches of the phenylpropanoid pathway, whereas the remaining proteins have been related to the plant response to both biotic and abiotic stresses. The comparison of candidate grape WRKYs involved in *STS* transcription with those characterized in other species (Fig. 3B) indicated both VviWRKY03 and VviWRKY43 as closely related to *Captis japonica* CjWRKY01, *Solanum tuberousum* StWRKY1 TFs and also to the grape VviWRKY52 (previously named WRKY1 by Marchive et al. 2007, 2013). CjWRKY01 has been shown to have a role in the transcriptional regulation of several structural genes involved in the biosynthesis of the alkaloid barberine (Kato et al. 2007) whereas the tomato StWRKY1 TF is involved in the regulation of hydroxycinnamic acid amid

(HCAA) biosynthetic genes and in the cell wall straightening upon *Plasmopara infestans* invasion (Yogendra et al. 2015). Overexpression of *VviWRKY1 (VviWRKY52)* in tobacco has been shown to improve resistance to pathogenic fungi such as *Phytium* and to oomycetes such as *Peronospora tabacina* (Marchive et al. 2007), whereas in grapevine it was associated with the transcriptional regulation of three genes putatively involved in the Jasmonic acid signalling pathway and in the reduced susceptibility to downy mildew (*Plasmopara viticola*) infection (Marchive et al. 2013).

VviWRKY24 is a putative orthologue of the Arabidopsis At*WRKY33* gene, known to be involved in many processes including heat and NaCl tolerance, redox homeostasis, resistance to *Botrytis cinerea* and *Pseudomonas syringae*, SA signaling, ethylene-JA-mediated cross-communication and camalexin biosynthesis (Birkenbihl et al. 2012). In grapevine VviWRKY24 (known as WRKY33 in the nomenclature introduced by Merz et al. 2015), is associated with an increased resistance to *P. viticola* infection in the susceptible cultivar (cv.) 'Shiraz' and seems to be functionally related to defense. Finally, VviWRKY53 is closely associated with SlWRKY73, which was found to transiently trans-activate a tomato terpene synthase (TPS) gene in *Nicotiana benthamiana* leaves (Spyropoulou et al. 2014).

Expression of selected *WRKY* genes correlates with *MYB14/15* and *STS* transcripts under biotic and abiotic stress

We further explored the tight relationship observed between *STS* and their candidate regulators using the datasets from which the GCNs were constructed. We extrapolated the expression patterns of *STSs*, *MYBs* and *WRKYs* from a subset of biotic stressed samples (Fig. 4), showing that most *STS* genes are induced upon a range of different biotic stresses including infection with the necrotrophic fungus *Botrytis cinerea*, the biotrophic powdery mildew (*Erisiphe necator*) and oomycetes such as downy mildew (*P. viticola*). Of particular interest was the transcriptional regulation of a subgroup of *STS* genes that form a small cluster on chromosome 10 (*STS1-6*). These genes showed a much lower induction in response to downy mildew infection in comparison to most of the other members of the *STS* gene family (which cluster in a 500 Kb region on chromosome 16). This supports the previous report of Vannozzi et al. (2012), who showed that members of this small cluster of *STS* genes on chromosome 10 genes were less responsive to *P. viticola* infection than *STS* genes on chromosome 16. However, Fig. 4 clearly shows that both sets of *STS* genes are equally responsive to other biotic stresses. No induction of *STSs* was observed in response to infection with GRSPaV (Grapevine rupestris stem pitting-associated virus) (Fig. 4). This is in agreement with the work of Gambino et al. (2012) who observed that genes

involved in stress and pathogen responses are downregulated in the presence of co-evolved viruses such as GRSPaV.

Looking at the transcriptional response of the selected R2R3-MYB and WRKY TFs, we observed a good correlation with *STS* transcription (Fig. 4). *MYB14*/*15* were induced whenever *STSs* were induced, as previously reported in Höll et al. (2013). Similarly, transcription of several *WRKY* genes also showed a high level of correlation with *STS* genes. This was particularly evident for *WRKY03*, *-43* and *-24*. The induction of *WRKY24* in response to biotic stress previously reported by Merz et al. (2015), who observed a strong up-regulation in leaves infected with downy mildew in the resistant cv. 'Regent'. A less clear relationship was observed between transcription of *STS* family members and *MYB13* or *WRKY53*. For example, both TF genes were down-regulated in powdery mildew-infected leaves of some grapevine accessions while the former is also down-regulated in the late stages of *Botrytis*-infected berries (*B. cinerea* S2, and S3; Blanco-Ulate et al. 2015). As suggested previously, MYB13 may be responsible for *STS* regulation under basal (non-stressed) conditions or to developmental transitions.

Under abiotic stress conditions, the correlation between transcription of *STSs* and the candidate TF regulators was less evident compared to biotic stress (Figure 5). Nonetheless, a clear induction was found under drought stress during the ripening of white berries, late véraison heat stress of berries, and UV-C irradiation in berry skins, and in response to hormone (i.e. Gibberellic acid) treatments in flowers.

To further validate the correlations observed in the GCNs and heatmaps, we analysed the transcript levels of a subset of WRKY candidates (i.e. *WRKY03*, *WRKY43, WRKY53)*, *MYB14* and *MYB15* TFs, and three highly responsive *STS*s (*STS29*, *STS41* and *STS48*), in cv. 'Pinot Noir' leaves exposed to wounding and UV-C treatments by qPCR (Fig. 6). As previously reported in Höll et al. (2013) since the grapevine *STS* family is composed of 48 closely related genes (Vannozzi et al. 2012, Parage et al. 2012), it was not possible to design sequence specific-primers for the detection of only one *STS* isoform. Therefore, primers STS41-F/R detect isoforms *STS41 &* 45, while the primers STS29-F/R detect isoforms *VvSTS25, 27 & 29*. The results of the qPCR analysis confirmed our GCN analysis, showing a marked co-induction between the *STS.*

In response to mechanical wounding the transcript level of *VvSTS29*, *-41* and *-48* gradually increased over a 48-hour period, reaching a peak at 48h. *STS29* was the *STS* member showing the highest induction in terms of normalized transcript level, showing a fold change (FC) of 2400 times higher respect to the unwounded leaf (T0) followed by *STS41* (FC ≈ 1400) and *STS48* (FC ≈ 750). Looking at the expression of *VvSTS* candidate TF regulators, both WRKY and R2R3-MYB TFs were induced under wound stress. Similar to what was observed by Höll et al. (2013), *MYB14* and *MYB15* were both induced upon stress reaching their peaks at 48 h. *MYB14*

reached higher values compared to *VviMYB15* although, looking at the fold change respect to the 0h time point, both TFs reach similar values at their peak (FC ≈ 60-80). *WRKY03* showed the highest and most significant induction reaching a peak at 48 h corresponding to a FC of 495. *WRKY43* and *WRKY53* showed a lower but progressive increase over the 48h time course, peaking at the last stage (FC= 61 and 115, respectively).

In the UV-C treatment, gene expression was plotted as a log2 fold change between UV-C treated and untreated leaf discs (Fig. 6). In the UV-C treatment, gene expression was plotted as a log2 fold change between treated (UV-C) and untreated (i.e. wounded) samples at the same time point (Fig. 6). Thus, it must be noted that the lower fold change values observed for UV-C treated samples shouldn't be ascribed to lower responsiveness of candidate genes to the irradiation treatment per se, but to the fact that the untreated samples already showed a very high expression for these genes. *STS29* and *STS48* reached their peaks of induction at 6h (FC ≈ 39 and 12 respectively), followed by a slight decrease at 24 h. *STS41* showed a gradual increase reaching its peak at 24h (FC ≈ 41). *WRKY03* reached the maximum induction at 3h (FC ≈ 3), maintained this level until 6h (FC=2.81) and then decreased at 24h (FC=1.94). *WRKY43* reached a first peak of fold change value at 3h (FC=6.93), followed by a slight decrease at 6 h with a fold change of over 4, then a higher peak at 24h (FC=18.49). A similar trend was observed for *WRKY53*, which reached a first peak of expression at 3h, followed by a slight decrease at 6h, and by a second higher peak at 24h (FC ≈ 5). *MYB14* showed a progressive increase in expression, reaching its peak at 24h (FC ≈ 5), whereas *MYB15* reached the maximum expression 3 h after the imposition of the stress, with a fold change of approximately 14, and maintained this level in the following hours. We also evaluated the effects of the wound and UVC stress treatments in a shorter time frame, i.e. within the first 10 hours after the stress imposition (Supplementary figure S2) conforming the induction of *VvSTSs*, *VviMYBs* and candidate *VviWRKY* TFs is coherent with what reported in Fig. 6 also at earlier time-points.

Singular and combinatorial roles of WRKY and R2R3-MYB transcription factors in STS regulation in grapevine

To assess whether WRKY TFs are able to regulate the transcription of *STS* genes in grapevine cells, we performed transient gene reporter assays using the *VviSTS29* gene promoter. We selected this gene because it belongs to the highly responsive stilbene synthase subgroup B and showed a high correlation with candidate *WRKYs*. The dual luciferase reporter assay has been used previously to functionally validate the role of many other transcriptional regulators of the flavonoid pathway, including VviMYB14 and VviMYB15 (Höll et al. 2013).

A ~1.2 Kb promoter fragment of *VviSTS29* gene isolated previously (Höll et al. 2013) was comprehensively screened for canonical MYB (i.e. type I – CNGTTR, II – TNGTTR, and IIG/AC-element – CCWAMC; where N=A/C/G/T, R=A/G, W=A/T, M=A/C) and WRKY (i.e. TTGACY; where Y=C/T) TFBS. A total of two, six, and two type I, II, and IIG MYB binding sites respectively and two WRKY TFBS were identified (Fig. 7A; Supplementary Table S4). Interestingly, the type IIG/AC-element TFBS was situated in close proximity (< ± 50 bp) with the two WRKY binding sites. Many studies have now established that functional combinatorial relationships between multiple TFBS are widespread across plant promoters, and this property play a key role in determining the transcriptional dynamics of organ-, tissue-, and/or stress-specific gene expression in plants (Vandepoele et al. 2006, Maruyama et al. 2012, Wong et al. 2017). Distance constraint (< ± 100 bp) between multiple TFBS is also essential for their functionality (VAndepoele et al. 2006) and are strong indicators of interacting TFs (Yu et al. 2006a, 2006b). Therefore, the co-occurrence of multiple MYB and WRKY TFBS and a strong distant constraint between them (< ± 100 bp) observed for STS29 promoter provides support for both singular and combinatorial control of *STS29* by MYB and WRKY TFs that may be potentially mediated by MYB and WRKY TF interaction.

To test for WRKY and MYB activation of the *VviSTS29* promoter, transient expression assays were conducted on cv. 'Chardonnay' berry suspension cell cultures using a dual reporter luciferase system as previously described (Höll et al. 2013). The *VviSTS29* promoter sequence was fused to the *Firefly LUCIFERASE* (*LUC*) gene and co-transfected in cells with candidate TFs. Candidate TFs were cloned into thepART7 vector (Gleave 1992) under the control a 35S promoter and transfected in cells as single or combined TFs (Fig. 7B-C). Chardonnay cell suspensions transiently expressing the *proSTS29:LUC* luciferase reporter construct showed significant increases in the *STS29* promoter activity of approximately 4-fold when co-transformed with Vvi*MYB14* and 5-fold when co-transformed with Vvi*MYB15*, in line with previous results (Höll et al. 2013). Of the candidate WRKY TFs tested, a statistically significant induction of Vvi*STS29* promoter activity was only observed in cells co-transfected with VviWRKY24, which led to a 4-fold increase in the luciferase activity. This induction of the Vvi*STS29* promoter by VviWRKY24 is comparable to the activation observed with VviMYB14 and VviMYB15.

None of the other candidate WRKY TFs analyzed were found to produce a statistically significant effect on the *VvSTS29* promoter activity. This includes VviWRKY52, which was not co-expressed with any *STS* genes in the combined GCN, and thus serves as a null candidate without evident roles in directly regulating *STS* expression including *STS29*. Despite this, we observed several interactions when WRKY and R2R3-MYB TFs were co-transfected (Fig. 7). A statistically significant increase in the *VvSTS29*p luciferase activity was observed when

VviMYB14 was transfected with VviWRKY03 leading to two-fold increase when compared to VviMYB14 alone, corresponding to an 8-fold increase compared to the control. This observation suggests a combinatorial effect of VviWRKY03 and VviMYB14 in the regulation of the pathway, or at least of this particular VviSTS member, which may be specific to the regulatory networks implicated in module 1 (Fig. 2). This observation also raises the question whether these MYB and WRKY proteins could interact. Similar results were observed in *Petunia hybrida*, where the WRKY transcription factor PH3 interacts with a MYB-bHLH-WD40 complex (MBW), constituted by PhPH4, PhAN1, and PhAN11 encoding for a MYB, a bHLH and a WD40, respectively, and activates downstream genes in multiple distinct pathways involved in flower pigmentation and seed development (Verweij et al. 2016). Stilbene biosynthesis in grapevine is spatially and developmentally regulated and additionally induced by many abiotic and biotic environmental cues, which needs a complex regulatory network. The combinatory regulation of *VviSTS29p* by VviMYB14 and VviWRKY03 and its induction by VviWRKY24 could be part of this network leading to fine adjustments of stilbene biosynthesis in respect to changing developmental and environmental conditions.

Concluding remarks

A systems-oriented study encompassing genome-wide gene co-expression (GCN) analysis, integrated GCN, phylogenetics, and DNA-binding motif analysis, was performed with the ultimate goal of identifying novel transcriptional regulators of the grapevine stilbene biosynthetic pathway. In this study, the use of the integrated TF–*STS* network has provided an added advantage of revealing additional co-expression relationships between transcription factors and *STS* genes that may have not been detected had only a single platform been used for GCN analysis (Wong et al. 2016, Wong and Matus, 2017). In Arabidopsis, formal assessments have shown that RNA-Seq GCN can be accurate, satisfying both biological and robust network topology properties, while revealing novel functional gene neighborhoods missed in microarray-based GCN (Giorgi et al. 2013).

The integrated TF–STS network analysis indicated a number of TFs belonging to different families, including WRKYs, MYBs and an ERF, that are putatively involved in the regulation of the grapevine *STS* multigenic family. Amongst the best candidate regulatory genes identified by this analysis was *VviMYB14*, belonging to the R2R3-MYB family, for which a role in the transcriptional regulation of at least two *STSs* has already been documented (Höll et al. 2013). This observation further validates the choice and validity of GCN analysis in gene function prediction used in this and other studies (Usadel et al. 2009). Amongst the candidate TFs inferred from the combined grapevine STS and TF GCN, we focused on members of the WRKY family which collectively showed the highest correlation with *STS* gene expression under a stringent connectivity threshold as well as the

well-documented roles of this TF family in the regulation of stress related genes in plants (reviewed in Jiang al. 2017). Most of the WRKY TFs found as co-expressed in our GCN analysis were found to be potential orthologues of genes already characterized in grapevine or in other plant species, involved in biotic and abiotic stress responses, in signalling pathways related to the response to exogenous stimuli, and in the biosynthesis of different families of secondary metabolites.

Detailed analysis was carried out on four *WRKY* genes (*WRKY3*, *WRKY24*, *WRKY43* and *WRKY53* according to the nomenclature proposed by Wang et al. 2014) based on their level of PCC correlation and on the number of interactions they showed with *STSs*. Generally, the observations obtained by the meta-analysis of two large gene expression compendia used in the GCN construction and the quantitative PCR analyses performed on stressed leaves (wounded and UV-C treated) confirmed that, together with *VviMYB14* and *VviMYB15*, these *WRKY TFs* were induced whenever *STSs* and *R2R3-MYBs* were induced. This observation further reinforces their coordinated regulation, especially under stress, and strongly suggests a role in the regulation of the stilbene biosynthetic pathway.

Functional validation of candidate WRKYs indicated both a singular and combinatorial role for several members. In particular, VvWRKY24, an orthologue of Arabidopsis WRKY33, was found to have a direct effect on the promoter activity of *VvSTS29*, independent of VvMYB14 and VvMYB15. The fact that stilbenes act as phytoalexins in grapevine and the phylogenetic relatedness between VviWRKY24 and AtWRKY33, suggests some similarities with the regulation of the PTI (pattern triggered immunity) response in Arabidopsis (Jiang et al. 2017). Interestingly, VviWRKY3, which had no effect on *STS29* promoter activity on its own, appeared to act synergistically with VviMYB14 to increase STS promoter activity. This observation, together with the presence of the type IIG/AC-element TFBS in close proximity (< ± 50 bp) with two WRKY binding sites within the *VvSTS29* promoter region supports the hypothesis of a protein-protein interaction between the MYB and WRKY TFs. Although a direct interaction between these two TF proteins is unlikely, it could be mediated by other "bridge" proteins such as WD40s and bHLHs as already observed in *Petunia* (Verweij et al. 2016). Validation of this hypothesis will require yeast-2-hybrid (Y2H) assays to investigate interactions between VviWRKY3 and VvMYB14 and to screen *prey* libraries with the aim of identifying potential "bridge" proteins.

In addition to the new insights into the regulatory roles of VviWRKY24 and VviWRKY3 in the regulation of the STS pathway, this study has also identified a large collection of other candidate TFs for future gene characterization studies. Validation of these candidates will require a combination of many different approaches including expression profiling experiments associated with chromatin immunoprecipitation, yeast-2-hybrid

assays to investigate protein-protein interactions and *in planta* functional assays to validate roles of these regulators in the grapevine stilbene pathway.

Materials and methods

Compilation of transcriptome datasets and gene expression analysis

Two separate transcriptome compendia were constructed: one based on microarray datasets (29K NimbleGen Grape Whole-genome platform) and another one with next-generation sequencing (RNA-Seq) datasets. Details regarding each dataset are available in Supplementary Table S1. For compiled microarray datasets, raw intensity data were summarized with *oligo* (Carvalho et al. 2010) using the robust multi-array average method in R (http://www.r-project.org). The final microarray dataset consists of RMA-normalized values across 356 conditions with biological replicates being averaged when present. For RNA-Seq datasets, raw paired-end or single-end fastq reads were first trimmed and quality filtered using Trimmomatic v0.36 (Bolger et al. 2014) with the following parameters; LEADING, TRAILING, SLIDINGWINDOW, MINLEN, and AVGQUAL of 20, 20, 4:20, 40, and 20, respectively. Trimmed reads were then aligned to the 12X v1 grapevine reference genome (Jaillon et al. 2007), count summarized, and FPKM transcript abundance estimated using HISAT2 v2.0.5 (Kim et al. 2015), featureCounts (Liao et al. 2014), and edgeR (Robinson et al. 2009), respectively using default settings. The final RNA-Seq expression dataset consists of expression estimates (log2 FPKM+1) across 236 conditions with biological replicates being averaged when present. Re-analysis of differential gene expression was performed using *limma* (Ritchie et al., 2015) and *DESeq2* (Love et al., 2014) for microarray and RNA-seq datasets, respectively. False discovery rate (FDR) < 0.05 and an absolute log2FC > 0.5 defines significant differential gene expression between contrasts (treatment/control) evaluated (See Supplementary table S1).

Gene co-expression network construction and statistical significance of reciprocal ranks

Construction of a mutual rank (MR; Obayashi et al. 2009) gene co-expression network (GCN) for the microarray and RNA-Seq transcriptome compendia was performed separately as previously reported (Wong et al. 2017 in R. The MR score for any two genes (i.e. gene A and gene B), is determined according to: $MR_{(AB)} = \sqrt{(Rank_{(A \rightarrow B)} \times Rank_{(B \rightarrow A)})}$, whereby $Rank_{(A \rightarrow B)}$ corresponds to the assigned ranking of gene B in a PCC -ordered (descending) list of gene A co-expressed genes, and *vice versa* for $Rank_{(B \rightarrow A)}$. The final order of each genes' co-expressed genes list is sorted by ascending MR scores, with smaller scores indicating strong and robust co-expression (Obayashi et al. 2009). The optimal size of each *STS* gene co-expression neighborhood, *k* to be considered for

the construction of the complete *STS* 'guide' co-expression modules was determined using two approaches. The first involves the inspection of the observed (complete *STS* GCN) and representative null PCC distribution at various *k* intervals of 100 to 1,000 (stepwise of 100). The null PCC distribution was first obtained by random sampling of 1,000 genes (Vandepoele et al. 2006). This sampling procedure is then repeated 100 times to obtain a representative null distribution. The second involves the establishment of statistical significant MR following the approach of Mutwil et al. (2011) which involves the analysis of MR distribution over 1,000 permutations of the original gene expression dataset. Both analyses were performed separately for respective microarray and RNA-Seq transcriptome compendia. Visualization of network modules was achieved using Cytoscape v3.3 (Shannon et al. 2003). Final aggregation of the modules in the two compendia was performed by merging node (degree) and edge (PCC) attributes to produce a final integrated network. Highly interconnected and modular structures in the integrated *STS*-correlated *TF-TF* subnetwork was identified with *GLay* (Su et al. 2010) implemented in Cytoscape.

Phylogeny, structural and protein analysis of candidate genes

Multiple sequence alignment (MSA) of 13 candidate WRKY genes, including *VviWRKY03* (VIT_01s0010g03930), *VviWRKY24* (VIT_08s0058g00690), *VviWRKY43* (VIT_14s0068g01770) and *VviWRKY53* (VIT_17s0000g05810) and the other forty-two WRKY TFs already characterized in other plant species, was inferred by using MUSCLE (http://www.ebi.ac.uk/Tools/msa/muscle/). Phylogenetic analyses were performed with MEGA software using the Neighbor-joining (NJ) algorithm and 1000 bootstrap iterations. The accessions of WRKY proteins considered in the analysis are as follows: *AaWRKY01* (FJ390842), *AtWRKY01* (NP_178565.1), *AtWRKY12* (AF404857), *AtWRKY16* (NM_180802.2), *AtWRKY18* (NM_119329.4), *AtWRKY22* (NM_116355.3), *AtWRKY23* (AY052647), *AtWRKY29* (NM_118486.6), *AtWRKY33* (AK226301), *AtWRKY40* (NM_106732.4), *AtWRKY44* (NM_129282), *AtWRKY46* (NM_130204.3), *AtWRKY50* (NM_122518.3), *AtWRKY51* (NM_125877.4), *AtWRKY52* (NM_001344604.1), *AtWRKY60* (NM_001335968.1), *CjWRKY01* (AB267401), *CrWRKY01* (HQ646368), *GaWRKY01* (AY507929), *HbWRKY01* (JF742559), *HbWRKY41* (GU372969), *MtSTP* (HM622066), *MtWRKY100577* (EU526033), *MtWRKY100630* (EU526034), *MtWRKY108715* (EU526035), *MtWRKY109669* (EU526036), *NbWRKY08* (AB445392), *OsWRKY13* (EF143611), *OsWRKY45* (AK066255), *OsWRKY53* (AB190436), *OsWRKY74* (XP_015651250.1), *OsWRKY76* (AK068337), *OsWRKY89* (AY781112), *PgWRKY01* (KR060074), *PqWRKY01* (JF508376), *PsWRKY01* (JQ775582), *PtrWRKY73* (Potri.013G153400.1), *SlWRKY73* (NM_001247873), *SpWRKY01* (AK320342), *TcWRKY01* (JQ250831), *VviWRKY01* (AY585679), *VviWRKY02* (AY596466). Length of protein sequences,

559 molecular weight (MW), theoretical isoelectric point (pI), protein instability index (II), aliphatic index (AI), and
560 grand average of hydropathicity (GRAVY) of *VviWRKY03*, *-24*, *-43*, and *-53* were calculated using Protparam
561 Expasy tool (http://web.expasy.org/protparam; Gasteiger et al. 2005).

562

563 **Mechanical wounding and UV-C stress treatments**

564 Leaf discs (10 mm diameter) were punched from healthy leaves detached from glasshouse-grown *V. vinifera* cv.
565 'Pinot Noir' vines. Discs were pooled from leaves of the same stage of development, based on leaf size and
566 nodal position, collected from a minimum number of three different potted vines. The punching of discs was
567 considered as a wounding treatment *per se*. Five discs randomly chosen from the pool were sampled at 0, 1, 3, 6,
568 24 and 48 h after wounding, incubated upside down on moist 3MM filter paper in large Petri dishes in the dark
569 at 22 °C until harvest, immediately frozen in liquid nitrogen and stored at -80 °C until RNA extraction. Control
570 discs (0 h) were collected from an unwounded leaf immediately following detaching from a healthy vine. The
571 UV-C treatment was carried out as described previously (Vannozzi et al. 2012), with discs irradiated with a 254
572 nm light source (0.36J cm^{-3}) at a distance of 10 cm for 10 min. Efficiency of the elicitation treatments under
573 different experimental conditions was determined histochemically by evaluating the intensity of auto-
574 fluorescence of discs mounted with the underside up in a lactic acid, glycerol and water mixture (1:1:1, v/v/v) on
575 glass slides under long-wave UV light (365 nm). The intensity of the observed blue fluorescence was correlated
576 with the quantity of resveratrol quantified in samples. Control discs (not elicited) were exposed to normal light
577 conditions. After treatment, all samples were incubated in the dark at 22 °C. Five discs were randomly chosen
578 from control and UV-C treatments at 0, 1, 3, 6, and 24 h, immediately frozen in liquid nitrogen, and stored at -80
579 °C until RNA extraction for expression analyses.

580

581 **Quantitative RT-PCR expression analysis of Group-B *STSs*, *CHSs*, *MYB14/15* and selected *WRKY* genes**
582 **in grapevine**

583 Expression analyses were carried out by quantitative RT-PCR using the "Fast SYBR® Green Master Mix" and
584 the StepOne^{TM} Plus Real-Time PCR System (Applied Biosystems). The samples were analyzed in three
585 technical replicates. Each 10 µl reaction contained 5 µl SYBR Green Master Mix, 0.6 µl of each primer, 1 µl
586 cDNA and 2.8 µl H_2O. The thermal cycling conditions used were 95 °C for 10 min followed by 40 cycles of: 95
587 °C for 15 s, 60 °C for 1 min., and 72 °C for 30 s, followed by a melt cycle with 1 °C increments from 55 to 96
588 °C. The selection of reference genes to normalize the cDNA represents a critical step in any quantitative RT-

PCR analysis. After testing its suitability, elongation factor EF1 (GenBank Accession no. AF176496) was selected for normalization of all samples analyzed. The expression of each target gene was calculated relative to the expression of elongation factor in each cDNA using StepOne™ Software version 2.1 (Applied Biosystems) to calculate normalized expression values (Yuan et al. 2006), observe melt profiles, extrapolate the concentration and measure primer pairs efficiencies. All oligonucleotide primer sequences are listed in Supplementary Table S5.

in silico cis-regulatory element screening of _VvSTS29_ promoter

The cloned *VvSTS29* promoter fragment (1.2 Kb fragment upstream of TSS) was scanned for the main R2R3-MYB (e.g. type I, CNGTTR; type II, TNGTTR; and type IIG/AC, CCWAMC) (Prouse and Campbell 2012 and WRKY (i.e. core W-box, TTGACY) TF binding sites (Eulgem et al. 2000), using regular expression functions in R for exact pattern match (with no mismatch allowed) along both + and – strands.

Cloning of _VviWRKY03_, _VviWRKY43_, and _VvWRKY53_ for dual reporter luciferase assays

The complete coding sequences of *VviWRKY3*, *VviWRKY43* and *VviWRKY53* were amplified from cv. 'Pinot Noir' cDNA obtained from UV-C irradiated grapevine leaves using proofreading Taq polymerase. Sequence specific primers (Supplementary Table S5) designed to the putative 5' and 3' UTRs of target genes were designed using Geneious R8 software on grapevine sequences downloaded from the grape Genome browser (http://genomes.cribi.unipd.it/grape). The generated PCR fragments were purified from agarose gels, cloned directly in pENTR/D TOPO gateway vector (ThermoFisher Scientific) and transferred into GW-pART7 vector to produce pART7-*VvWRKY3*, pART7-*VvWRKY43* and pART7-*VvWRKY53* constructs, where WRKY factors were under control of a 35S promoter. The vector pART7[30] was previously modified into a gateway compatible destination vector by using the Gateway® Vector Conversion System (ThermoFisher Scientific®, according to the manufacture protocol; Poschet G., unpublished data). Cloning of pART7-*VviWRYK24* (former *VviWRKY33*) was described by Merz et al. (2015). Reporter constructs carrying firefly luciferase and the promoter sequences of *VvSTS29* gene, together with pART-*MYB14* and pART-*MYB15* constructs were previously described in Höll et al. (2013).

Transient transfection experiments and dual luciferase assay

Transient promoter-reporter gene assays were performed using cell suspension cultures obtained from *V. vinifera* cv Chardonnay and Pinot noir petiole callus culture as previously described (Bogs et al. 2007, Walker et al.

2007). The Dual Luciferase assay was modified according to Czemmel et al. (2009). The Renilla luciferase pRluc was utilized as an internal control in each transfection experiment (Horstmann et al. 2004). Transfection experiments were conducted using single or combined effectors. All transfection experiments were repeated 3 to 5 times, with three technical replicates per experiment. Promoter activity was measured as a fold change compared to control. Mean values of firefly and *Renilla* luciferase ratios are reported as relative luciferase activity with error bars indicating SE.

Funding

This work was supported by the Cariparo Foundation (Cariparo Starting Grants) and the Department of Agronomy, Food, Natural resources, Animals, and Environment (DAFNAE), University of Padova.

Disclosure

The authors have no conflicts of interest to declare.

References

Ali, K., Maltese, F., Choi, Y.H., and Verpoorte, R. (2010) Metabolic constituents of grapevine and grape-derived products. *Phytochem. Rev*. 9, 357–78.

Aoki, Y., Okamura, Y., Tadaka, S., Kinoshita, K., and Obayashi, T. (2016) ATTED-II in 2016: A plant coexpression database towards lineage-specific coexpression. *Plant Cell Physiol*. 57: e5.

Becatti, E., Genova, G., Ranieri, A., and Tonutti, P. (2014) Postharvest treatments with ethylene on Vitis vinifera (cv Sangiovese) grapes affect berry metabolism and wine composition. *Food Chem*. 159: 257–266.

Belhadj, A., Telef, N., Cluzet, S., Bouscaut, J., Corio-Costet, M.F., and M??rillon, J.M. (2008) Ethephon elicits protection against Erysiphe necator in grapevine. *J Agric Food Chem*. 56: 5781–5787.

Birkenbihl, R.P., Diezel, C., and Somssich, I.E. (2012) Arabidopsis WRKY33 Is a Key Transcriptional Regulator of Hormonal and Metabolic Responses toward Botrytis cinerea Infection. *PLANT Physiol*. 159: 266–285.

Blanco-Ulate, B., Amrine, K.C., Collins, T.S., Rivero, R.M., Vicente, A.R., Morales-Cruz, A., et al. (2015) Developmental and metabolic plasticity of white-skinned grape berries in response to Botrytis cinerea during noble rot. *Plant Physiol*. 169: 2422-2443.

Bogs, J., Jaffe, F.W., Takos, A.M., Walker, A.R., and Robinson, S.P. (2007) The Grapevine Transcription Factor VvMYBPA1 Regulates Proanthocyanidin Synthesis during Fruit Development. *PLANT Physiol*. 143: 1347–1361.

Bolger, A.M., Lohse, M., and Usadel, B. (2014) Trimmomatic: A flexible trimmer for Illumina sequence data. *Bioinformatics*. 30: 2114–2120.

Canaguier, A., Grimplet, J., Di Gaspero, G., Scalabrin, S., Duchêne, E., Choisne, N., et al. (2017) A new version of the grapevine reference genome assembly (12X.v2) and of its annotation (VCost.v3). *Genomics Data*. 14: 56–62.

Carvalho, B.S., and Irizarry, R.A. (2010) A framework for oligonucleotide microarray preprocessing. *Bioinformatics*. 26: 2363–2367.

Cavallini, E., Matus, J.T., Finezzo, L., Zenoni, S., Loyola, R., Guzzo, F., et al. (2015) The Phenylpropanoid Pathway Is Controlled at Different Branches by a Set of R2R3-MYB C2 Repressors in Grapevine. *Plant Physiol*. 167: 1448–1470.

Chezem, W.R., and Clay, N.K. (2016) Regulation of plant secondary metabolism and associated specialized cell development by MYBs and bHLHs. *Phytochemistry*. 131: 26–43.

Chong, J., Poutaraud, A., and Hugueney, P. (2009) Metabolism and roles of stilbenes in plants. *Plant Sci.* 143–55.

Corso, M., Vannozzi, A., Maza, E., Vitulo, N., Meggio, F., Pitacco, A., et al. (2015) Comprehensive transcript profiling of two grapevine rootstock genotypes contrasting in drought susceptibility links the phenylpropanoid pathway to enhanced tolerance. *J Exp Bot*. 66: 5739–5752.

Czemmel, S., Stracke, R., Weisshaar, B., Cordon, N., Harris, N.N., Walker, A.R., et al. (2009) The Grapevine R2R3-MYB Transcription Factor VvMYBF1 Regulates Flavonol Synthesis in Developing Grape Berries. *PLANT Physiol*. 151: 1513–1530.

672 Davies, K.M., and Schwinn, K.E. (2003) Transcriptional regulation of secondary metabolism. *Funct. Plant Biol.*
673 30: 913–25.

674 Eulgem, T., Rushton, P.J., Robatzek, S., and Somssich, I.E. (2000) The WRKY superfamily of plant
675 transcription factors. *Trends Plant Sci.* 5: 199–206.

676 Eulgem, T., Rushton, P.J., Robatzek, S., and Somssich, I.E. (2000) The WRKY superfamily of plant
677 transcription factors. *Trends Plant Sci.* 5: 199-206.

678 Fabres, P.J., Collins, C., Cavagnaro, T.R., and Rodríguez López, C.M. (2017) A Concise Review on Multi-
679 Omics Data Integration for Terroir Analysis in Vitis vinifera. *Front Plant Sci*. 8.

680 Fang, L., Hou, Y., Wang, L., Xin, H., Wang, N., and Li, S. (2014) Myb14, a direct activator of STS, is
681 associated with resveratrol content variation in berry skin in two grape cultivars. *Plant Cell Rep*. 33: 1629–1640.

682 Fujimoto, S.Y. (2000) Arabidopsis Ethylene-Responsive Element Binding Factors Act as Transcriptional
683 Activators or Repressors of GCC Box-Mediated Gene Expression. *PLANT CELL ONLINE*. 12: 393–404.

684 Gambino, G., Cuozzo, D., Fasoli, M., Pagliarani, C., Vitali, M., Boccacci, P., et al. (2012) Co-evolution between
685 Grapevine rupestris stem pitting-associated virus and Vitis vinifera L. leads to decreased defence responses and
686 increased transcription of genes related to photosynthesis. *J Exp Bot*. 63: 5919–5933.

687 Gasteiger, E., Hoogland, C., Gattiker, A., Duvaud, S., Wilkins, M.R., Appel, R.D., et al. (2005) Protein
688 Identification and Analysis Tools on the ExPASy Server. In *The Proteomics Protocols Handbook*. pp. 571–607.

689 Giorgi, F.M., Del Fabbro, C., and Licausi, F. (2013) Comparative study of RNA-seq- and Microarray-derived
690 coexpression networks in Arabidopsis thaliana. *Bioinformatics*. 29: 717–724.

691 Gleave, A.P. (1992) A versatile binary vector system with a T-DNA organisational structure conducive to
692 efficient integration of cloned DNA into the plant genome. *Plant Mol Biol*. 20: 1203–1207.

693 Hichri, I., Heppel, S.C., Pillet, J., Léon, C., Czemmel, S., Delrot, S., et al. (2010) The basic helix-loop-helix
694 transcription factor MYC1 is involved in the regulation of the flavonoid biosynthesis pathway in grapevine. *Mol*
695 *Plant*. 3: 509–523.

696 Höll, J., Vannozzi, A., Czemmel, S., D'Onofrio, C., Walker, A.R., Rausch, T., et al. (2013) The R2R3-MYB
697 Transcription Factors MYB14 and MYB15 Regulate Stilbene Biosynthesis in Vitis vinifera. *Plant Cell*. 25:
698 4135–4149.

699 Horstmann, V., Huether, C.M., Jost, W., Reski, R., and Decker, E.L. (2004) Quantitative promoter analysis in
700 Physcomitrella patens: A set of plant vectors activating gene expression within three orders of magnitude. *BMC*
701 *Biotechnol*. 4: 13.

702 Hu, Y., Han, Y.-T., Zhang, K., Zhao, F.-L., Li, Y.-J., Zheng, Y., et al. (2016) Identification and expression
703 analysis of heat shock transcription factors in the wild Chinese grapevine (Vitis pseudoreticulata). *Plant Physiol*
704 *Biochem PPB / Société Fr Physiol végétale*. 99: 1–10.

705 Huang, J., Vendramin Alegre, S., Shi, L., and McGinnis, K. (2017) Construction and Optimization of Large
706 Gene Co-expression Network in Maize Using RNA-Seq Data. *Plant Physiol*. pp.00825.2017.

707 Jaillon, O., Aury, J.M., Noel, B., Policriti, A., Clepet, C., Casagrande, A., et al. (2007) The grapevine genome
708 sequence suggests ancestral hexaploidization in major angiosperm phyla. *Nature*. 449: 463–467.

709 Jeandet, P., Delaunois, B., Conreux, A., Donnez, D., Nuzzo, V., Cordelier, S., et al. (2010) Biosynthesis,
710 metabolism, molecular engineering, and biological functions of stilbene phytoalexins in plants. *BioFactors*. 36:
711 331–341.

712 Jiang, J., Ma, S., Ye, N., Jiang, M., Cao, J., and Zhang, J. (2017) WRKY transcription factors in plant responses
713 to stresses. *J. Integr. Plant Biol.* 59: 86–101.

714 Jin, J., Tian, F., Yang, D.C., Meng, Y.Q., Kong, L., Luo, J., et al. (2017) PlantTFDB 4.0: Toward a central hub
715 for transcription factors and regulatory interactions in plants. *Nucleic Acids Res*. 45: D1040–D1045.

716 Kato, N., Dubouzet, E., Kokabu, Y., Yoshida, S., Taniguchi, Y., Dubouzet, J.G., et al. (2007) Identification of a
717 WRKY protein as a transcriptional regulator of benzylisoquinoline alkaloid biosynthesis in Coptis japonica.
718 *Plant Cell Physiol*. 48: 8–18.

719 Kim, D., Langmead, B., and Salzberg, S.L. (2015) HISAT: A fast spliced aligner with low memory
720 requirements. *Nat Methods*. 12: 357–360.

721 Liao, Y., Smyth, G.K., and Shi, W. (2014) FeatureCounts: An efficient general purpose program for assigning
722 sequence reads to genomic features. *Bioinformatics*. 30: 923–930.

723 Licausi, F., Giorgi, F.M., Zenoni, S., Osti, F., Pezzotti, M., and Perata, P. (2010) Genomic and transcriptomic
724 analysis of the AP2/ERF superfamily in Vitis vinifera. *BMC Genomics*. 11: 719.

725 Love, M.I., Huber, W., and Anders, S. (2014) Moderated estimation of fold change and dispersion for RNA-seq
726 data with DESeq2. *Genome Biol*. 15: 550.

727 Loyola, R., Herrera, D., Mas, A., Wong, D.C.J., Höll, J., Cavallini, E., et al. (2016) The photomorphogenic
728 factors UV-B RECEPTOR 1, ELONGATED HYPOCOTYL 5, and HY5 HOMOLOGUE are part of the UV-B
729 signalling pathway in grapevine and mediate flavonol accumulation in response to the environment. *J Exp Bot*.
730 67: 5429–5445.

731 Marchive, C., Léon, C., Kappel, C., Coutos-Thévenot, P., Corio-Costet, M.F., Delrot, S., et al. (2013) Over-
732 Expression of VvWRKY1 in Grapevines Induces Expression of Jasmonic Acid Pathway-Related Genes and
733 Confers Higher Tolerance to the Downy Mildew. *PLoS One*. 8: 1–8.

734 Marchive, C., Mzid, R., Deluc, L., Barrieu, F., Pirrello, J., Gauthier, A., et al. (2007) Isolation and
735 characterization of a Vitis vinifera transcription factor, VvWRKY1, and its effect on responses to fungal
736 pathogens in transgenic tobacco plants. *J Exp Bot*. 58: 1999–2010.

737 Maruyama, K., Todaka, D., Mizoi, J., Yoshida, T., Kidokoro, S., Matsukura, S., et al. (2012) Identification of
738 cis-acting promoter elements in cold-and dehydration-induced transcriptional pathways in arabidopsis, rice, and
739 soybean. *DNA Res*. 19: 37–49.

740 Matus, J.T., Cavallini, E., Loyola, R., Höll, J., Finezzo, L., Dal Santo, S., et al. (2017) A group of grapevine
741 MYBA transcription factors located in chromosome 14 control anthocyanin synthesis in vegetative organs with
742 different specificities compared with the berry color locus. *Plant J*. 91: 220–236.

743 Merz, P.R., Moser, T., Höll, J., Kortekamp, A., Buchholz, G., Zyprian, E., et al. (2015) The transcription factor
744 VvWRKY33 is involved in the regulation of grapevine (Vitis vinifera) defense against the oomycete pathogen
745 Plasmopara viticola. *Physiol Plant*. 153: 365–380.

746 Mizoi, J., Shinozaki, K., and Yamaguchi-Shinozaki, K. (2012) AP2/ERF family transcription factors in plant
747 abiotic stress responses. *Biochim Biophys*. 1819: 86–96.

748 Mutwil, M., Klie, S., Tohge, T., Giorgi, F.M., Wilkins, O., Campbell, M.M., et al. (2011) PlaNet: Combined
749 Sequence and Expression Comparisons across Plant Networks Derived from Seven Species. *Plant Cell*. 23: 895–
750 910.

751 Mutwil, M., Klie, S., Tohge, T., Giorgi, F.M., Wilkins, O., Campbell, M.M., et al. (2011) PlaNet: Combined
752 Sequence and Expression Comparisons across Plant Networks Derived from Seven Species. *Plant Cell*. 23: 895–
753 910.

754 Nakai, K., and Horton, P. (1999) PSORT: A program for detecting sorting signals in proteins and predicting
755 their subcellular localization. *Trends Biochem. Sci.* 24: 34–6.

756 Obayashi, T., and Kinoshita, K. (2009) Rank of correlation coefficient as a comparable measure for biological
757 significance of gene coexpression. *DNA Res*. 16: 249–260.

758 Obayashi, T., and Kinoshita, K. (2010) Coexpression landscape in ATTED-II usage of gene list and gene
759 network for various types of pathways. *J. Plant Res.* 123: 311-319.

760 Pangeni, R., Sahni, J.K., Ali, J., Sharma, S., and Baboota, S. (2014) Resveratrol: review on therapeutic potential
761 and recent advances in drug delivery. *Expert Opin Drug Deliv*. 11: 1285–1298.

762 Parage, C., Tavares, R., Réty, S., Baltenweck-Guyot, R., Poutaraud, A., Renault, L., et al. (2012) Structural,
763 functional, and evolutionary analysis of the unusually large stilbene synthase gene family in grapevine. *Plant*
764 *Physiol*. 160: 1407–19.

765 Prouse, M.B., and Campbell, M.M. (2012) The interaction between MYB proteins and their target DNA binding
766 sites. *Biochim. Biophys. Acta.* 1819: 67-77.

767 Ritchie, M.E., Phipson, B., Wu, D., Hu, Y., Law, C.W., Shi, W., et al. (2015) limma powers differential
768 expression analyses for RNA-sequencing and microarray studies. *Nucleic Acids Res*. 43: e47.

769 Rivière, C., Pawlus, A.D., and Mérillon, J.-M. (2012) Natural stilbenoids: distribution in the plant kingdom and
770 chemotaxonomic interest in Vitaceae. *Nat Prod Rep*. 29: 1317.

771 Robinson, M.D., McCarthy, D.J., and Smyth, G.K. (2010) edgeR: a Bioconductor package for differential
772 expression analysis of digital gene expression data. *Bioinformatics*. 26: 139–40.

773 Scharf, K.-D., Berberich, T., Ebersberger, I., and Nover, L. (2012) The plant heat stress transcription factor (Hsf)
774 family: structure, function and evolution. *Biochim Biophys Acta*. 1819: 104–19.

775 Serna, L. (2007) bHLH proteins know when to make a stoma. *Trends Plant Sci.* 12(11): 483–5.

776 Shannon, P., Markiel, A., Ozier, O., Baliga, N.S., Wang, J.T., Ramage, D., et al. (2003) Cytoscape: A software
777 Environment for integrated models of biomolecular interaction networks. *Genome Res*. 13: 2498–2504.

778 Shen, T., Wang, X.-N., and Lou, H.-X. (2009) Natural stilbenes: an overview. *Nat Prod Rep*. 26: 916.

779 Spyropoulou, E.A., Haring, M.A., and Schuurink, R.C. (2014) RNA sequencing on Solanum lycopersicum
780 trichomes identifies transcription factors that activate terpene synthase promoters. *BMC Genomics*. 15: 402.

781 Su, G., Kuchinsky, A., Morris, J.H., States, D.J., and Meng, F. (2010) GLay: community structure analysis of
782 biological networks. *Bioinformatics*. 26: 3135–7.

783 Sun, X., Matus, J.T., Wong, D.C.J., Wang, Z., Chai, F., Zhang, L., et al. (2018) The GARP/MYB-related grape
784 transcription factor AQUILO improves cold tolerance and promotes the accumulation of raffinose family
785 oligosaccharides. *Journal of Experimental Botany*. *Accepted*.

786 Toledo-Ortiz, G. (2003) The Arabidopsis Basic/Helix-Loop-Helix Transcription Factor Family. *PLANT CELL*
787 *ONLINE*. 15: 1749–1770.

788 Tsai, H.Y., Ho, C.T., and Chen, Y.K. (2017) Biological actions and molecular effects of resveratrol,
789 pterostilbene, and 3'-hydroxypterostilbene. *J. Food Drug Anal.* 25: 134–47.

790 Usadel, B., Obayashi, T., Mutwil, M., Giorgi, F.M., Bassel, G.W., Tanimoto, M., et al. (2009) Co-expression
791 tools for plant biology: opportunities for hypothesis generation and caveats. *Plant, Cell Environ.* 32(12): 1633–
792 51.

793 Vandepoele, K., Casneuf, T., and Van de Peer, Y. (2006) Identification of novel regulatory modules in
794 dicotyledonous plants using expression data and comparative genomics. *Genome Biol*. 7: R103.

795 Vannozzi, A., Dry, I.B., Fasoli, M., Zenoni, S., and Lucchin, M. (2012) Genome-wide analysis of the grapevine
796 stilbene synthase multigenic family: genomic organization and expression profiles upon biotic and abiotic
797 stresses. *BMC Plant Biol*. 12: 130.

798 Velasco, R., Zharkikh, A., Troggio, M., Cartwright, D.A., Cestaro, A., Pruss, D., et al. (2007) A high quality
799 draft consensus sequence of the genome of a heterozygous grapevine variety. *PLoS One*. 2.

800 Verweij, W., Spelt, C.E., Bliek, M., de Vries, M., Wit, N., Faraco, M., et al. (2016) Functionally Similar WRKY
801 Proteins Regulate Vacuolar Acidification in Petunia and Hair Development in Arabidopsis. *Plant Cell*. 28: 786–
802 803.

803 Vitulo, N., Forcato, C., Carpinelli, E., Telatin, A., Campagna, D., D'Angelo, M., et al. (2014) A deep survey of
804 alternative splicing in grape reveals changes in the splicing machinery related to tissue, stress condition and
805 genotype. *BMC Plant Biol*. 14: 99.

806 Walker, A.R., Lee, E., Bogs, J., McDavid, D.A.J., Thomas, M.R., and Robinson, S.P. (2007) White grapes arose
807 through the mutation of two similar and adjacent regulatory genes. *Plant J*. 49: 772–785.

808 Wang, M., Vannozzi, A., Wang, G., Liang, Y.-H., Tornielli, G.B., Zenoni, S., et al. (2014) Genome and
809 transcriptome analysis of the grapevine (Vitis vinifera L.) WRKY gene family. *Hortic Res*. 1: 14016.

810 Weiskirchen, S., and Weiskirchen, R. (2016) Resveratrol: How Much Wine Do You Have to Drink to Stay
811 Healthy? *Adv Nutr An Int Rev J*. 7: 706–718.

812 Wisecaver, J.H., Borowsky, A.T., Tzin, V., Jander, G., Kliebenstein, D.J., and Rokas, A. (2017) A Global
813 Coexpression Network Approach for Connecting Genes to Specialized Metabolic Pathways in Plants. *Plant Cell*.
814 29: 944–959.

815 Wong, D.C.J., and Matus, J.T. (2017) Constructing Integrated Networks for Identifying New Secondary
816 Metabolic Pathway Regulators in Grapevine: Recent Applications and Future Opportunities. *Front Plant Sci*. 8.

817 Wong, D.C.J., Lopez Gutierrez, R., Gambetta, G.A., and Castellarin, S.D. (2017) Genome-wide analysis of cis-
818 regulatory element structure and discovery of motif-driven gene co-expression networks in grapevine. *DNA Res*.
819 24: 311–326.

820 Wong, D.C.J., Schlechter, R., Vannozzi, A., Höll, J., Hmmam, I., Bogs, J., et al. (2016) A systems-oriented
821 analysis of the grapevine R2R3-MYB transcription factor family uncovers new insights into the regulation of
822 stilbene accumulation. *DNA Res*. 23: 451–466.

823 Wong, D.C.J., Sweetman, C., and Ford, C.M. (2014) Annotation of gene function in citrus using gene expression
824 information and co-expression networks. *BMC Plant Biol*. 14: 186.

825 Wong, D.C.J., Sweetman, C., Drew, D.P., and Ford, C.M. (2013) VTCdb: A gene co-expression database for the
826 crop species Vitis vinifera (grapevine). *BMC Genomics*. 14: 882.

827 Yogendra, K.N., Kumar, A., Sarkar, K., Li, Y., Pushpa, D., Mosa, K.A., et al. (2015) Transcription factor
828 StWRKY1 regulates phenylpropanoid metabolites conferring late blight resistance in potato. *J Exp Bot*. 66:
829 7377–7389.

830 Yu, X., Lin, J., Masuda, T., Esumi, N., Zack, D.J., and Qian, J. (2006) Genome-wide prediction and
831 characterization of interactions between transcription factors in Saccharomyces cerevisiae. *Nucleic Acids Res*.
832 34: 917–927.

833 Yu, X., Lin, J., Zack, D.J., and Qian, J. (2006) Computational analysis of tissue-specific combinatorial gene
834 regulation: Predicting interaction between transcription factors in human tissues. *Nucleic Acids Res*. 34: 4925–
835 4936.

836 Yuan, J.S., Reed, A., Chen, F., and Stewart, C.N. (2006) Statistical analysis of real-time PCR data. *BMC*
837 *Bioinformatics*. 7: 85.

838 Zhang, Y., and Wang, L. (2005) The WRKY transcription factor superfamily: Its origin in eukaryotes and
839 expansion in plants. *BMC Evol Biol*. 3: 5.

840

841

842

843

844

845

846

847

848

849

850 **Tables**

851 **Table 1.** List of all the TFs co-expressed with *VvSTS* genes (degree ≥ 5) represented in the GCN.

ID	Vitis Name	Family/subfamily	Degree	Function	Reference
Shared interaction module					
VIT_07s0005g03340	*VviMYB14*	R2R3-MYB / S2	74	STS regulation	Höll et al., 2013
VIT_08s0007g08750	*VviHsfB3a*	HSF / A	51	unknown	Hu et al., 2016
VIT_01s0010g03930	*VvWRKY3*	WRKY / IIc	41	unknown	Wang et al., 2014
VIT_01s0026g01730	*VvWRKY2*	WRKY / IIb	39	unknown	Wang et al., 2014
VIT_11s0016g02070	-	bHLH	38	unknown	
VIT_14s0068g01770	*VvWRKY43*	WRKY / IIc	36	unknown	Wang et al., 2014
VIT_08s0058g00690	*VvWRKY24*	WRKY / I	29	unknown	Wang et al., 2014
VIT_06s0004g00020	*VvNAC44*	NAC / S3	32	unknown	Wang et al., 2013
VIT_07s0005g03220	*VvERF098*	ERF/AP2 / IX	29	unknown	Licausi et al., 2010
VIT_12s0055g00340	*VvWRKY39*	WRKY / IIb	22	unknown	Wang et al., 2014
VIT_10s0116g01200	*VvWRKY29*	WRKY / IIb	14	unknown	Wang et al., 2014
VIT_00s1352g00010	*VviMYB148*	R2R3-MYB / S14	11	unknown	Wong et al., 2016
VIT_19s0027g00860	*VvNAC31*	NAC / S6	7	unknown	Wang et al., 2014
VIT_19s0085g00050	*VviMYB139*	R2R3-MYB / S3	5	unknown	Wong et al., 2016
RNAseq interaction module					
VIT_10s0003g01600	*VvWRKY30*	WRKY / IIe	34	unknown	Wang et al., 2014
VIT_17s0000g05810	*VvWRKY53*	WRKY / IIb	26	unknown	Wang et al., 2014
VIT_05s0077g00500	*VviMYB108A*	R2R3-MYB / S20	11	unknown	Wong et al., 2016
VIT_06s0061g00780	*C2H2*	C2H2	11	unknown	
VIT_09s0002g01190	*VviSHR3*	GRAS	10	unknown	Grimplet et al., 2016
VIT_15s0021g01600	-	ERF/AP2	10	unknown	Licausi et al., 2010
VIT_06s0004g04990	*VviLISCL2*	GRAS	7	unknown	Grimplet et al., 2016
VIT_15s0021g01610	-	ERF/AP2	6	unknown	Licausi et al., 2010
VIT_01s0150g00120	*VvERF112*	ERF/AP2 - X	5	unknown	Licausi et al., 2010
Microarray interaction module					
VIT_18s0072g00260	*VvERF114*	ERF/AP2 - X	29	unknown	Licausi et al., 2010
VIT_12s0028g00860	*VvNAC36*	NAC / S6	26	unknown	Wang et al., 2014
VIT_07s0031g01980	*VvERF113*	ERF/AP2 - X	22	unknown	Licausi et al., 2010
VIT_05s0049g01020	*VviMYB15*	R2R3-MYB / S2	15	STS regulation	Höll et al., 2013
VIT_04s0069g00970	*VvWRKY11*	WRKY / IIc	9	unknown	Wang et al., 2014
VIT_17s0000g00200	-	ERF/AP2	9	unknown	Licausi et al., 2010
VIT_02s0025g00420	*VvWRKY4*	WRKY / IIe	6	unknown	Wang et al., 2014
VIT_05s0049g01010	*VviMYB13*	R2R3-MYB / S2	5	STS regulation	Wong et al. 2016

852

853

854

Figures

Figure 1. Integrated gene co-expression network of grapevine stilbene synthase (*STS*) and transcription factors (*TFs*), obtained by integrating two subnetworks generated from microarray and RNA-Seq data, respectively. Each network was acquired by selecting the top200 ranking genes for each *STS* gene and filtering only those accession encoding for transcription factors based on Plant TFdb. The size of the TF nodes is proportional to the number of edges (i.e. the number of *STS* a particular TF is correlated with). The thickness of edges is proportional to the Pearson Correlation Coefficient (PCC). Nodes showing degree (number of edges) lower than 5 were excluded. Different TF families are represented by different colors.

Figure 2. Integrated *STS*-correlated *TF-TF* gene co-expression network. The TFs prioritized in the STS-TF top200 MR GCN were considered for highlighting their reciprocal relationships in term of co-expression. The size of the TF nodes is proportional to the number of edges, i.e. the number of *VvSTS* members that particular TF is correlated with. The thickness of edges is proportional to the Pearson Correlation Coefficient (PCC).

Figure 3. (A) Phylogenetic relationships of WRKY proteins from grapevine and Arabidopsis. The deduced proteins were aligned with MUSCLE and phylogenetic analyses were performed with MEGA software using the Neighbor-joining (NJ) algorithm and 1000 bootstrap iterations. WRKYs identified in the CGN analysis are indicated in red; (B) Phylogenetic tree obtained by multiple sequence alignment (MSA) of candidate WRKY genes together with other forty-two WRKY TFs already characterized in grapevine and in other plant species; (C) Length of protein sequences, molecular weight (MW), theoretical isoelectric point (pI), protein instability index (II), aliphatic index (AI), and grand average of hydropathicity (GRAVY) of candidate WRKYs were calculated using Protparam Expasy tool.

Figure 4. Gene expression heat map of stress responsiveness of the complete grapevine *STS* gene family, together with *VviMYB13*/*14*/*15* and the candidate *WRKY* genes *VviWRKY3*, *VviWRKY24*, *VviWRKY43* and *VviWRKY53*. A subset of samples representing biotic stress conditions was extrapolated from transcriptome compendia. Significantly up-regulated and down-regulated genes are indicated with varying intensities. False discovery rate (FDR) < 0.05 and an absolute log2FC > 0.5 defines significant differential gene expression between contrasts (treatment/control) evaluated (marked with *)

Figure 5. Heat map showing the expression of the whole *STS* gene family and of *VviMYB13*/*14*/*15*, *VviWRKY3*, *VviWRKY24*, *VviWRKY43* and *VviWRKY53* genes in a subset of samples extrapolated from transcriptome compendia representing abiotic stresses. Significantly up-regulated and down-regulated genes are indicated with

varying intensities. False discovery rate (FDR) < 0.05 and an absolute log2FC > 0.5 defines significant differential gene expression between contrasts (treatment versus control, marked with *).

Figure 6. Quantitative RT-PCR analysis of grapevine *STSs*, *R2R3-MYB* and candidate *VvWRKY* transcript accumulation in response to mechanical wounding and UV-C irradiation. Transcript levels were normalized to the expression of elongation factor *EF1-a* and plotted as $\log_2$ (fold change). Fold change for wounded discs was calculated relative to the untreated sample (0 h), whereas fold change for UV-C–treated discs was obtained by calculating the ratio between treated (UV-C) and untreated (i.e., wounded discs) samples at the same time point. The experiment was repeated twice with similar results. Data show the results of one of these experiments. Bars indicate SE of three technical replicates.

Figure 7. Transient expression in *V. vinifera* cv Chardonnay suspension cell culture following particle bombardment. Specific promoters linked to a *Firefly* luciferase gene were co-bombarded into cells with pART7-TF constructs. The Firefly luciferase activity was normalized with the *Renilla reniformis* luciferase activity, under control of a 35S promoter. For normalization of all data to the background activity of the *STS29* promoter, the empty pART7 vector was co-transformed with the *STS29* promoter::luciferase construct and used as negative control. A) Canonical MYB and WRKY TF binding sites (TFBS) in the cv "Shiraz" *VviSTS29* 1.2 Kb region used for luciferase assays. A total of two, six, and two type I, II, and IIG MYB binding sites respectively and two WRKY TFBS were identified; B) Dual reporter luciferase assays performed with singular MYB or WRKY effectors; C) Dual reporter luciferase assays performed with combined effectors (MYBs + WRKYs). Results were obtained from 3 to 5 independent experiments and mean averaged. The method currently being used to discriminate among the means is Fisher's least significant difference (LSD) procedure.

Supplementary material

Supplementary figure S1. Distribution of Pearson correlation coefficients (PCC) in the observed and random (A) microarray and (B) NGS *STS* gene co-expression network at different top *k* thresholds. Observed PCC distribution in (A) and (B) is represented as purple and red boxplots, respectively. Random PCC distribution in (A) and (B) is represented as green and cyan boxplots, respectively. Outlier PCC values in (A) and (B) are removed for clarity. Distribution of statistically significant mutual ranks in the global (C) microarray (D) NGS gene co-expression network at different significance level intervals ($0.05 > P\text{-}value > 0.001$). Scores are expressed as $-\log10(P\text{-}value)$.

Supplementary Figure S2. Quantitative RT-PCR analysis of grapevine *STSs*, *R2R3-MYB* and candidate *VvWRKY* transcript accumulation in response to mechanical wounding and UV-C irradiation within the first 10 h after treatment. Transcript levels were normalized to the expression of elongation factor *EF1-a* and plotted as $\log_2$ (fold change). Fold change for wounded discs was calculated relative to the untreated sample (0 h), whereas fold change for UV-C–treated discs was obtained by calculating the ratio between treated (UV-C) and untreated (i.e., wounded discs) samples at the same time point. Data show the results of one of these experiments. Bars indicate SE of three technical replicates.

Supplementary Table S1. Table summarizing the metadata used in the GCN construction indicating SRA ID, publication year, title, references, and number of assays.

Supplementary Table S2. List of the top 200 MR-ranked genes for each *VvSTS* member in both microarray and RNA-Seq compendia.

Supplementary Table S3. List of all the TFs co-expressed with *VvSTS* genes. Accessions highlighted in red represent TF with degree < 5 not reported in the main text (Table 1, Figure 1, Figure 2).

Supplementary Table S4. Distribution of canonical MYB and WRKY TF binding sites (TFBS) in the promoter fragment of *VviSTS29*.

Supplementary Table S5. List of oligonucleotides used in this study.

929

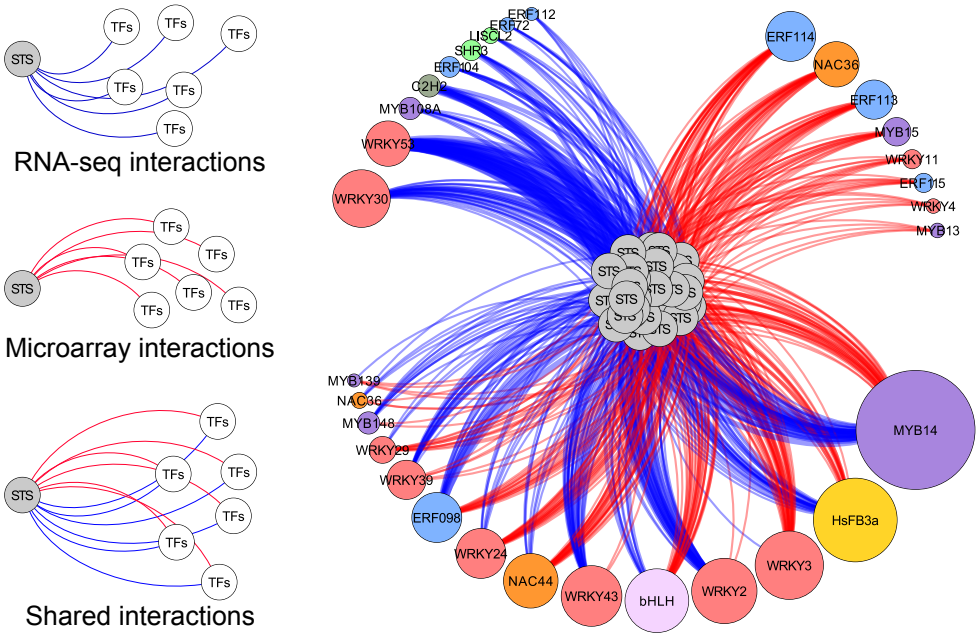
STS
TFs
RNA-seq interactions
Microarray interactions
Shared interactions
ERF112
ERF72
LISCL2
SHR3
ERF104
C2H2
MYB108A
WRKY53
WRKY30
ERF114
NAC36
ERF113
MYB15
WRKY11
ERF115
WRKY4
MYB13
MYB139
NAC36
MYB148
WRKY29
WRKY39
ERF098
WRKY24
NAC44
WRKY43
bHLH
WRKY2
WRKY3
HsFB3a
MYB14
STS
MYB
HSF
GRAS
WRKY
bHLH
ERF
NAC
C2H2

930

931

931

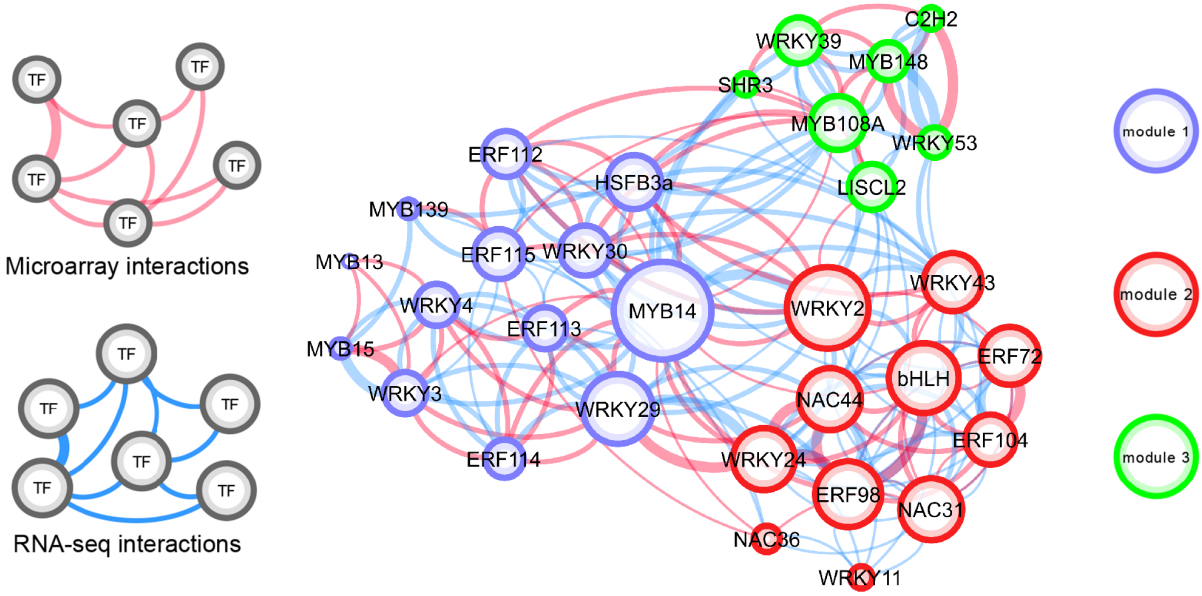
TF
Microarray interactions
RNA-seq interactions
C2H2
WRKY39
MYB148
SHR3
MYB108A
WRKY53
ERF112
HSFB3a
LISCL2
MYB139
MYB13
ERF115
WRKY30
WRKY4
MYB14
WRKY2
WRKY43
ERF113
MYB15
ERF72
bHLH
WRKY3
NAC44
WRKY29
ERF104
ERF114
WRKY24
ERF98
NAC31
NAC36
WRKY11
module 1
module 2
module 3

932

933

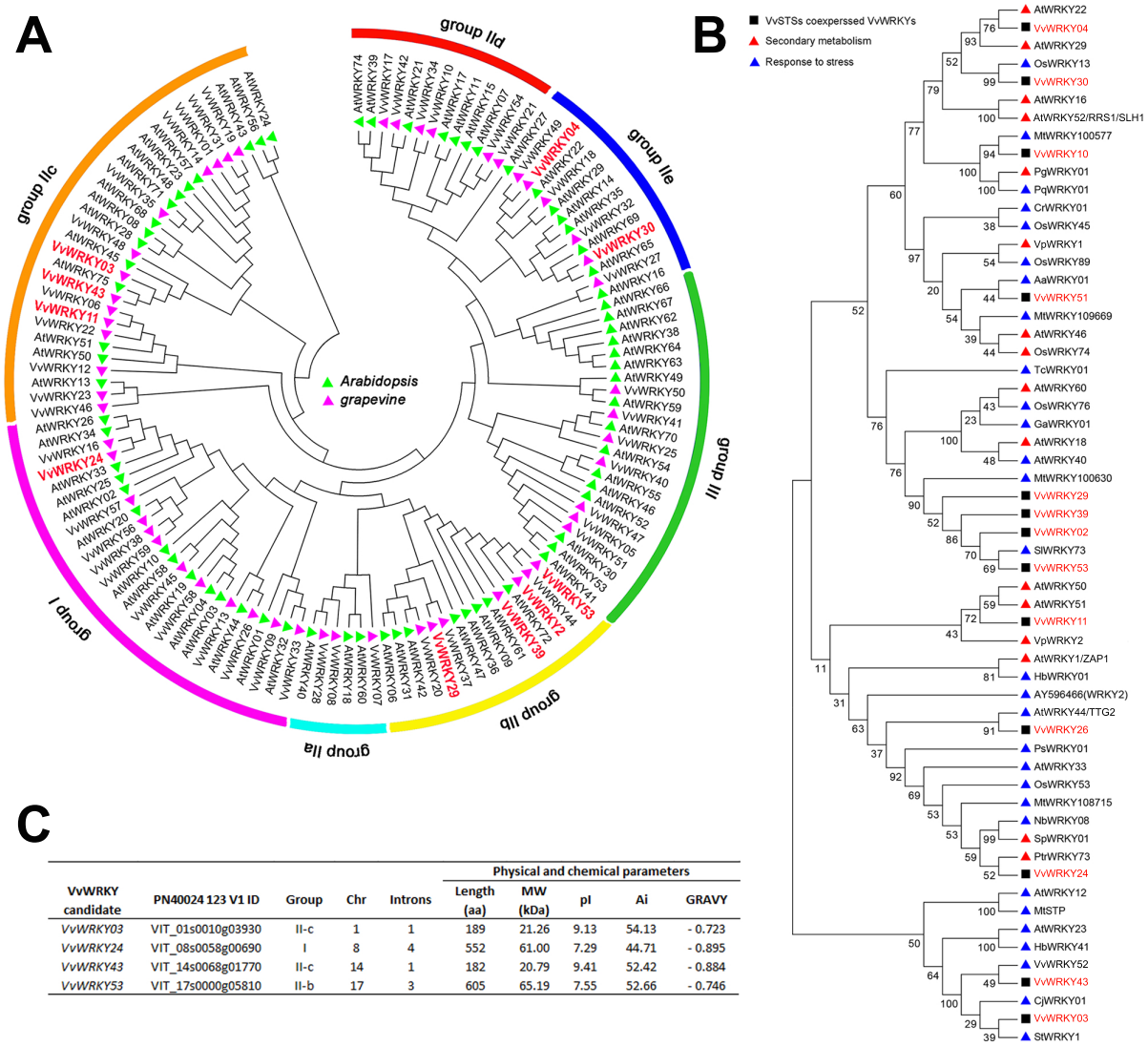

C

VvWRKY candidate	PN40024 123 V1 ID	Group	Chr	Introns	Physical and chemical parameters				
					Length (aa)	MW (kDa)	pI	Ai	GRAVY
VvWRKY03	VIT_01s0010g03930	II-c	1	1	189	21.26	9.13	54.13	- 0.723
VvWRKY24	VIT_08s0058g00690	I	8	4	552	61.00	7.29	44.71	- 0.895
VvWRKY43	VIT_14s0068g01770	II-c	14	1	182	20.79	9.41	52.42	- 0.884
VvWRKY53	VIT_17s0000g05810	II-b	17	3	605	65.19	7.55	52.66	- 0.746

934

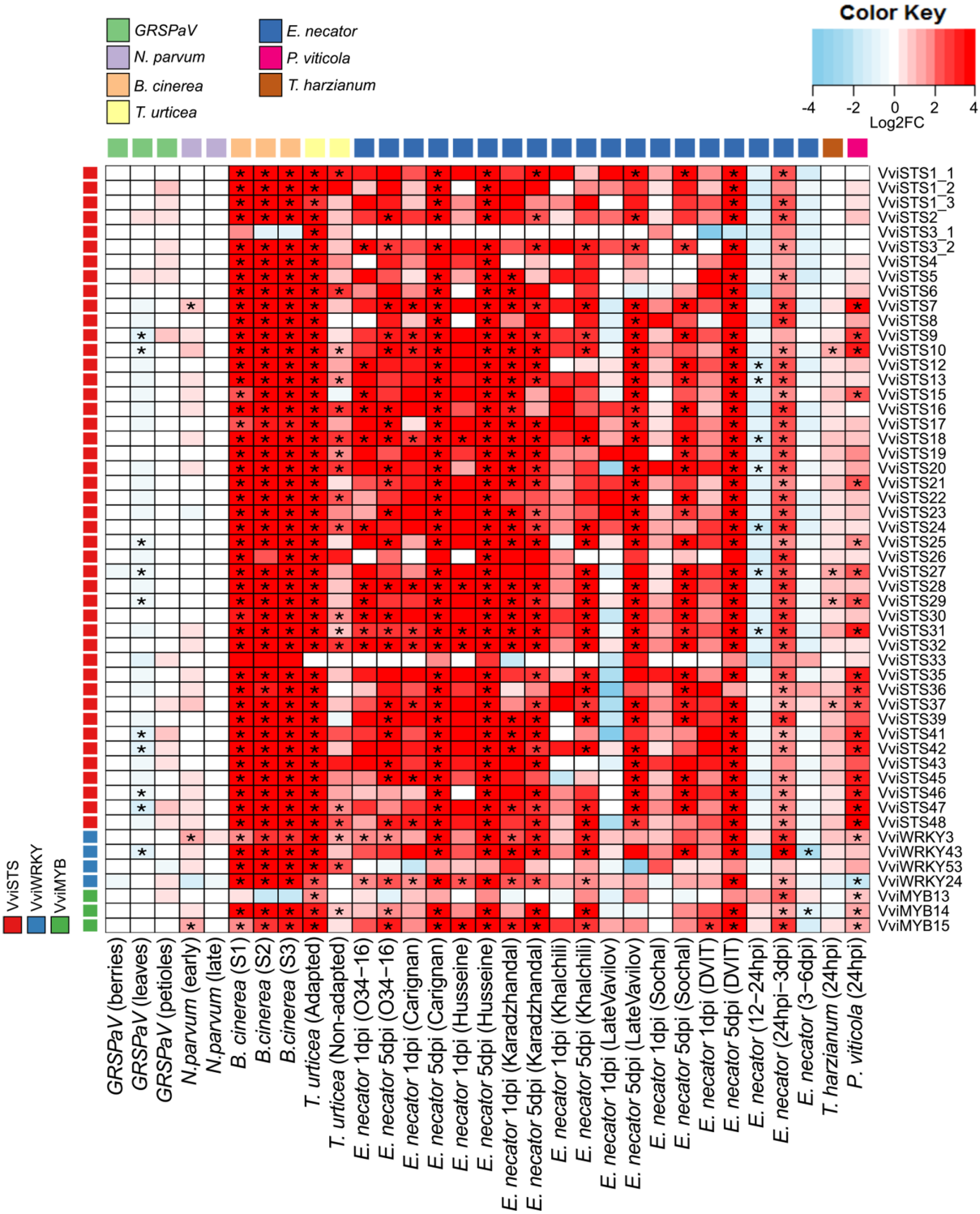
GRSPaV
N. parvum
B. cinerea
T. urticea
E. necator
P. viticola
T. harzianum
Color Key
-4
-2
0
2
4
Log2FC
ViSTS
ViWRKY
ViMYB
VviSTS1_1
VviSTS1_2
VviSTS1_3
VviSTS2
VviSTS3_1
VviSTS3_2
VviSTS4
VviSTS5
VviSTS6
VviSTS7
VviSTS8
VviSTS9
VviSTS10
VviSTS12
VviSTS13
VviSTS15
VviSTS16
VviSTS17
VviSTS18
VviSTS19
VviSTS20
VviSTS21
VviSTS22
VviSTS23
VviSTS24
VviSTS25
VviSTS26
VviSTS27
VviSTS28
VviSTS29
VviSTS30
VviSTS31
VviSTS32
VviSTS33
VviSTS35
VviSTS36
VviSTS37
VviSTS39
VviSTS41
VviSTS42
VviSTS43
VviSTS45
VviSTS46
VviSTS47
VviSTS48
VviWRKY3
VviWRKY43
VviWRKY53
VviWRKY24
VviMYB13
VviMYB14
VviMYB15
GRSPaV (berries)
GRSPaV (leaves)
GRSPaV (petioles)
N.parvum (early)
N.parvum (late)
B. cinerea (S1)
B.cinerea (S2)
B.cinerea (S3)
T. urticea (Adapted)
T. urticea (Non-adapted)
E. necator 1dpi (O34−16)
E. necator 5dpi (O34−16)
E. necator 1dpi (Carignan)
E. necator 5dpi (Carignan)
E. necator 1dpi (Husseine)
E. necator 5dpi (Husseine)
E. necator 1dpi (Karadzhandal)
E. necator 5dpi (Karadzhandal)
E. necator 1dpi (Khalchili)
E. necator 5dpi (Khalchili)
E. necator 1dpi (LateVavilov)
E. necator 5dpi (LateVavilov)
E. necator 1dpi (Sochal)
E. necator 5dpi (Sochal)
E. necator 1dpi (DVIT)
E. necator 5dpi (DVIT)
E. necator (12−24hpi)
E. necator (24hpi−3dpi)
E. necator (3−6dpi)
T. harzianum (24hpi)
P. viticola (24hpi)

937

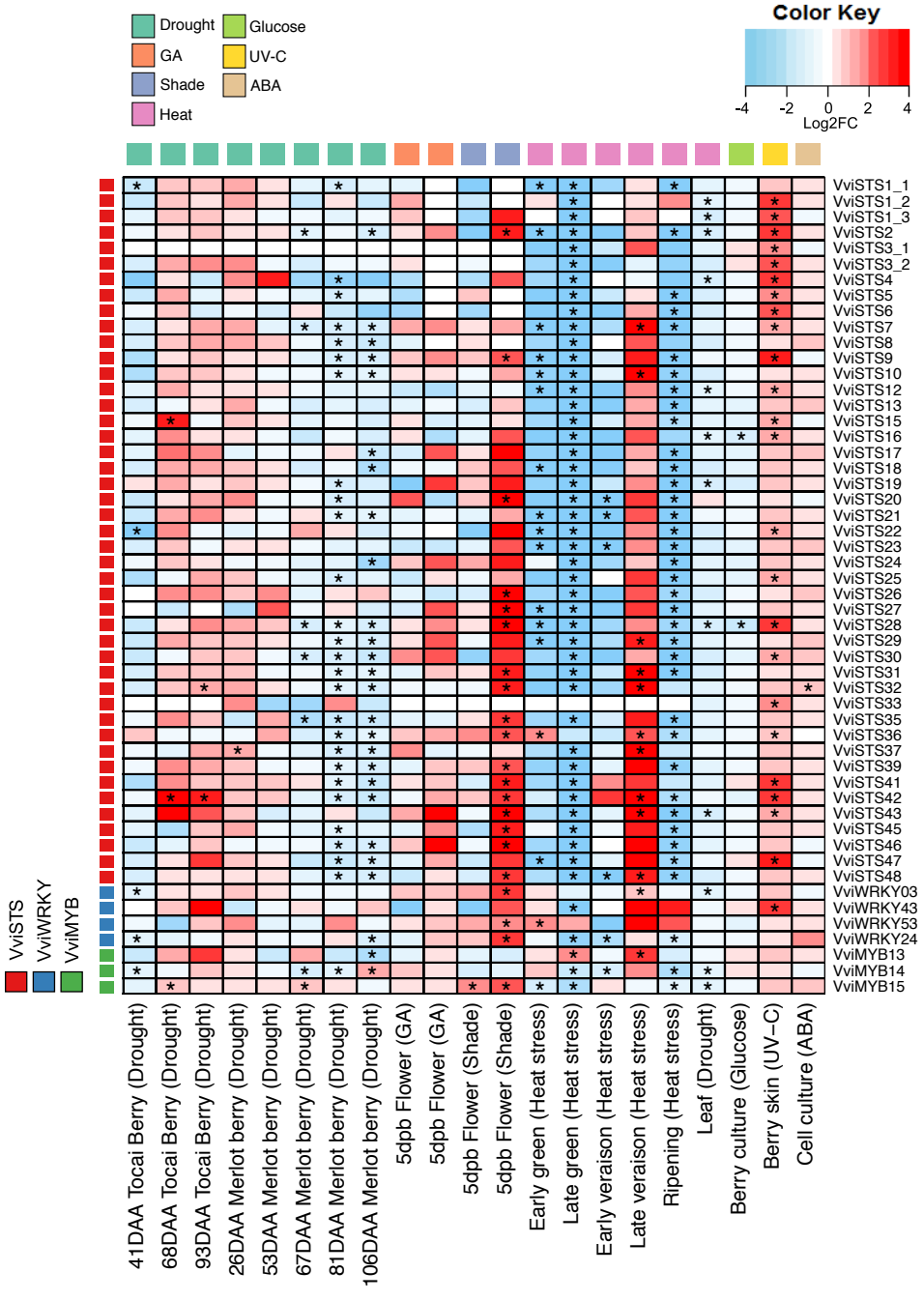
Drought
Glucose
GA
UV-C
Shade
ABA
Heat
Color Key
-4
-2
0
2
4
Log2FC
VviSTS
VviWRKY
VviMYB
VviSTS1_1
VviSTS1_2
VviSTS1_3
VviSTS2
VviSTS3_1
VviSTS3_2
VviSTS4
VviSTS5
VviSTS6
VviSTS7
VviSTS8
VviSTS9
VviSTS10
VviSTS12
VviSTS13
VviSTS15
VviSTS16
VviSTS17
VviSTS18
VviSTS19
VviSTS20
VviSTS21
VviSTS22
VviSTS23
VviSTS24
VviSTS25
VviSTS26
VviSTS27
VviSTS28
VviSTS29
VviSTS30
VviSTS31
VviSTS32
VviSTS33
VviSTS35
VviSTS36
VviSTS37
VviSTS39
VviSTS41
VviSTS42
VviSTS43
VviSTS45
VviSTS46
VviSTS47
VviSTS48
VviWRKY03
VviWRKY43
VviWRKY53
VviWRKY24
VviMYB13
VviMYB14
VviMYB15
41DAA Tocai Berry (Drought)
68DAA Tocai Berry (Drought)
93DAA Tocai Berry (Drought)
26DAA Merlot berry (Drought)
53DAA Merlot berry (Drought)
67DAA Merlot berry (Drought)
81DAA Merlot berry (Drought)
106DAA Merlot berry (Drought)
5dpb Flower (GA)
5dpb Flower (GA)
5dpb Flower (Shade)
5dpb Flower (Shade)
Early green (Heat stress)
Late green (Heat stress)
Early veraison (Heat stress)
Late veraison (Heat stress)
Ripening (Heat stress)
Leaf (Drought)
Berry culture (Glucose)
Berry skin (UV−C)
Cell culture (ABA)

938

939

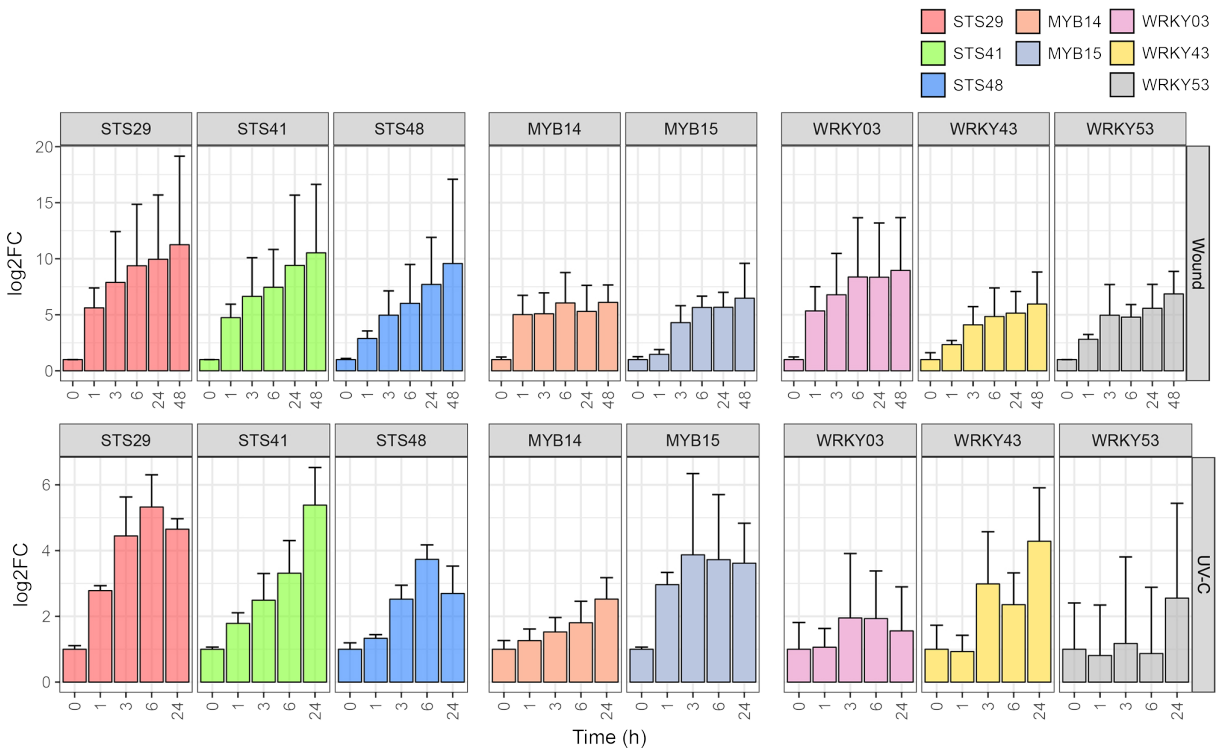
STS29
STS41
STS48
MYB14
MYB15
WRKY03
WRKY43
WRKY53
Wound
UV-C
log2FC
Time (h)

940

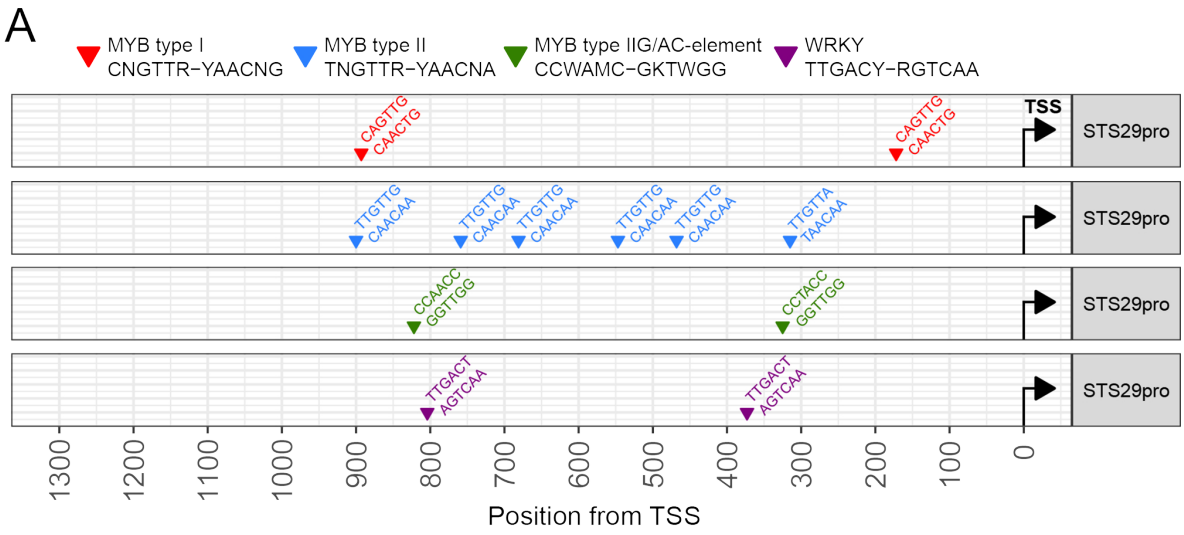
A
MYB type I
CNGTTR-YAACNG
MYB type II
TNGTTR-YAACNA
MYB type IIG/AC-element
CCWAMC-GKTWGG
WRKY
TTGACY-RGTCAA
TSS
STS29pro
CAGTTG
CAACTG
TTGTTG
CAACAA
TTGTTA
TAACAA
CCAACC
GGTTGG
CCTACC
GGTTGG
TTGACT
AGTCAA
1300
1200
1100
1000
900
800
700
600
500
400
300
200
100
0
Position from TSS

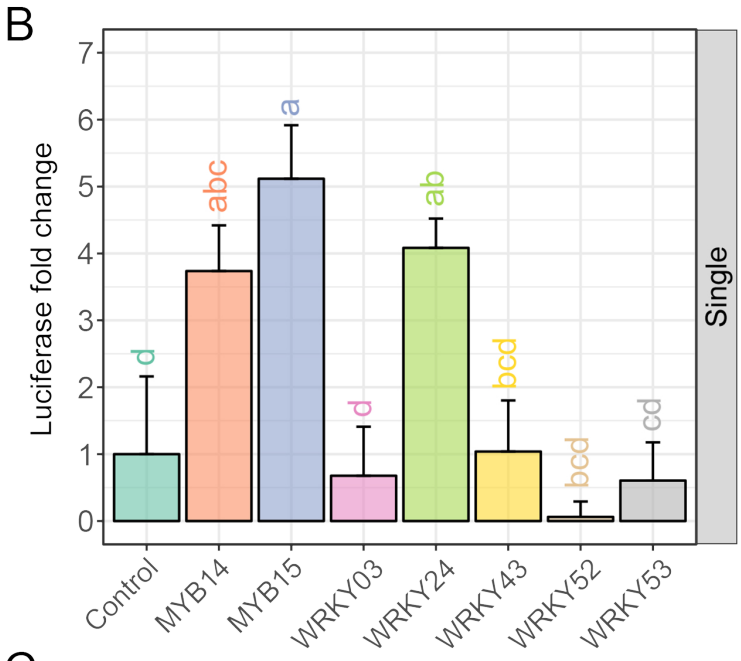
B
Luciferase fold change
Single
Control
MYB14
MYB15
WRKY03
WRKY24
WRKY43
WRKY52
WRKY53
d
abc
a
d
ab
bcd
bcd
cd

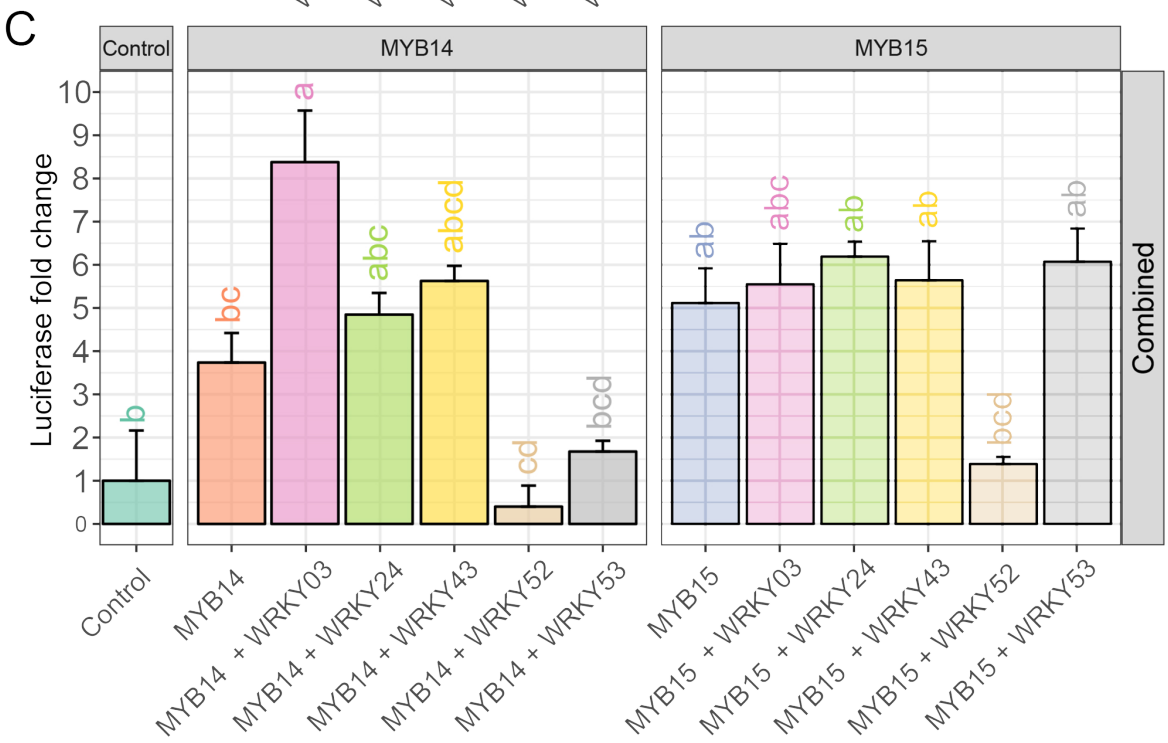
C
Control
MYB14
MYB15
Luciferase fold change
Combined
b
bc
a
abc
abcd
cd
bcd
ab
abc
ab
ab
bcd
ab
MYB14 + WRKY03
MYB14 + WRKY24
MYB14 + WRKY43
MYB14 + WRKY52
MYB14 + WRKY53
MYB15 + WRKY03
MYB15 + WRKY24
MYB15 + WRKY43
MYB15 + WRKY52
MYB15 + WRKY53

941